UNIVERSITÁ DEGLI STUDI DI MILANO

GRADUATE SCHOOL IN PHARMACOLOGICAL SCIENCES

Department of Medical Biotechnologies and Translational Medicine
Ph.D. course in Pharmacological Sciences
Cycle XXVII

Adult Sod1 G93R zebrafish model develops hallmark features of ALS and displays neuromuscular junctions defects and spinal neurons hyperexcitability at early developmental stages

Sector of study: BIO/14

Doctoral thesis of:
Lorena BENEDETTI
Matricola n° R09563

TUTOR:
Dr. Maura FRANCOLINI
COORDINATOR:
Chiar.mo Prof. Alberto PANERAI

Academic Year 2013-2014

INDEX

LIST OF ABBREVIATIONS

Common abbreviations are not shown.
Of note, the International System of Units was applied throughout this study.

A	Alanine
AChR	Nicotinic acetylcholine receptor
AcTub	Acetylated tubulin
AD	Autosomal dominant
Aif1	Allograft inflammatory factor 1
ALS	Amyotrophic lateral sclerosis
ALS2	Alsin
AMO	Antisense morpholino oligonucleotides
AMPAR	α-Amino-3-hydroxy-5-methyl-4-isoxazolepropionic acid receptor
ANG	Angiogenin
AR	Autosomal recessive
Arg	Arginine
ASF1/SF2	Alternative splicing factor 1/ pre-mRNA-splicing factor SF2
ATP	Adenosine triphosphate
ATXN2	Ataxin 2
a.u.	Arbitrary units
BSA	Bovine serum albumin
C	Cysteine
CaP	Caudal primary motor neuron
CHMP2B	Charged multivesicular body protein 2b
Ci-VSP	*Ciona intestinalis* voltage sensor-containing phosphatase
CMT	Charcot-Marie-Tooth disease
CNS	Central nervous system
CoPA	Commissural primary ascending interneuron
CPMP	Committee for Proprietary Medicinal Products
CRISPR	Clustered regularly interspaced short palindromic repeats
Cu	Copper
C9ORF72	Chromosome 9 open reading frame 72
D	Aspartic acid
DCTN1	Dynactin subunit 1
DENN	Differentially expressed in normal and neoplasia
DNA	Deoxyribonucleic acid
dNTP	Deoxynucleoside triphosphate
dpf	Days post fertilization
E	Glutamic acid
EAAT1	Astrocytic excitatory amino acid transporter 1
EAAT2	Astrocytic excitatory amino acid transporter 2
EDTA	Ethylenediaminetetraacetic acid
e.g.	For example
ELP3	Elongator complex protein 3
ER	Embryonic slow red muscle fibers
ESCRT	Endosomal sorting complexes required for transport
EW	Embryonic fast white fibers
FALS	Familial amyotrophic lateral sclerosis
FDA	Food and drug administration
FF	Fast fatigable motor neurons
FIG4	Factor-induced gene or Polyphosphoinositide phosphatase
FR	Fatigue resistant motor neurons

FRET	Fluorescence resonance energy transfer
FUS	Fused in sarcoma
G	Glycine
GABA	γ-Aminobutyric acid
GFAP	Glial fibrillary acidic protein
GLAST	Glutamate Aspartate Transporter
Gln	Glycine
GLT1	Glial Glutamate Transporter 1
GluR2	Subunit 2 of the AMPA receptor
GTP	Guanosine-5'-triphosphate
H	Histidine
HAA	Height at anterior of anal fin
HNRNPA1	Heterogeneous nuclear ribonucleoprotein A1
HNRNPA2B1	Heterogeneous nuclear ribonucleoproteins A2/B1
hpf	Hours post fertilization
HSP	Hereditary spastic paraplegia
HSR	Heat shock stress response
I	Isoleucine
IBA1	Ionized calcium binding adaptor molecule 1
IC	Ipsilateral caudal interneuron
i.e.	That is
IFN-γ	Interferon-γ
IGF1	Insulin growth factor 1
IL	Interleukin
I_{NaP}	Persistent (non-inactivating) sodium current
iPSC	Induced pluripotent stem cell
K	Lysine
kb	Kilobase
LMN	Lower motor neuron
LOCP	Length from the operculum to the caudal peduncle
m	Mutant
MBR	Metal binding region
MHLW	Ministry of Health, Labor and Welfare
MiP	Middle primary motor neuron
mKO_k	Monomeric Kusabira Orange fluorescent protein faster-maturating
MN	Motor neuron
MND	Motor neuron disease
mRNA	Messenger Ribonucleic acid
mSod1	Mutant G93R Sod1overexpressing zebrafish
MTR3	Matrin 3
mUKG	Monomeric Umi-Kinoko green fluorescent protein
N	Asparagine
NEFH	Neurofilament, heavy polypeptide
NMDAR	N-methyl-D-aspartate receptor
NMJ	Neuromuscular junction
NO	Nitric oxide
OPTN	Optineurin
ORF	Open reading frame
P	Postnatal day
PBS	Phosphate buffer saline
PFN1	Profilin1
PLS	Primary lateral sclerosis
PMA	Progressive muscular atrophy
PMN	Primary motor neuron

PMT	Photomultiplier
Q	Glutamine
QY	Quantum yield
R	Arginine
r	Repeated
RNA	Ribonucleic acid
ROS	Reactive oxygen species
RoP	Rostral primary motor neuron
RT	Room temperature
S	Serine
SALS	Sporadic amyotrophic lateral sclerosis
SETX	Senataxin
SHG	Second-harmonic generation
SL	Standard length
SLC1A2	Solute carrier family 1 member 2
SMN	Secondary motor neuron
SOD1	Superoxide dismutase 1
SPG11	Spastic paraplegia 11
SQSTM1	Sequestosome 1
SV2A	Synaptic vesicle glycoprotein 2A
T	Threonine
TALEN	Transcription activator-like effector nucleases
TARDBP	Transactive-region DNA-binding protein 43
TDP-43	Transactive response DNA-binding protein 43
TEM	Transmission electron microscope
TNFα	Tumor necrosis factor alpha
UAL	Unbranched axonal length
UBQLN2	Ubiquilin 2
UMN	Upper motor neuron
V	Valine
VaP	Variable primary motor neuron
VAPB	Vesicle-associated membrane protein-associated protein B
VCP	Valosin-containing protein
VeLD	Ventrolateral descending interneuron
Vps54	Vacuolar protein sorting 54
Vs	Versus
VSD	Voltage sensing domain
wt	Wild-type
wtSod1	wild-type Sod1 overexpressing Zebrafish
WTL	Wild-type-like
XD	X-linked dominant
Zn	Zinc
α-Btx	α-Bungarotoxin
ε	Extinction coefficient

SUMMARY

Amyotrophic Lateral Sclerosis (ALS) is an adult-onset neurodegenerative disease characterized by selective and progressive loss of motor neurons in the spinal cord, brain stem and motor cortex. Approximately 12% of familial and 1% of sporadic cases of ALS are associated to mutations in the gene coding for the antioxidant enzyme Cu-Zn Superoxide Dismutase type 1 (SOD1).

The scope of this project was to precisely investigate the typical hallmarks of ALS in the transgenic zebrafish models expressing the Sod1 mutation G93R and wild-type Sod1, in order to propose zebrafish as an animal model for the study of the disease. In this study, we have performed the detailed characterization of ALS features occurring in the adult transgenic zebrafish and we have exploited the great advantages given by zebrafish embryos and larvae as *in vivo* models to study the presymptomatic course of the disease.

Adult Sod1 G93R zebrafish recapitulate major ALS hallmarks

We characterized two stable transgenic zebrafish lines overexpressing the zebrafish Sod1 gene and regulatory sequences: a line expressing the wild-type form of Sod1 (wtSod1) and a mutant line (mSod1) where the Sod1 gene was mutated by changing the glycine 93 to arginine (G93R): a mutation that has been identified in human familial form of ALS. The two lines selected express the transgene at similar moderate levels in all tissues especially in the brain, in the spinal cord and in the muscle.

Although 12 months old mSod1 and wtSod1 zebrafish do not present alterations in the body weight and macroscopic anatomy in comparison with non-transgenic fish (Ctrl), the monitoring of the spontaneous locomotor activity reveals a significant reduction in the distance travelled and a significant increase in the time spent at resting by mSod1 fish compared to Ctrl zebrafish.

The evaluation of the presence of the typical ALS phenotype in the spinal cord and in the lateral muscle of adult zebrafish trunk was performed with histological analyses. Twelve months old fish were divided into segments using fins as standard anatomical references in order to study the disease features along the entire body of the animals. The comparative histological examination reveals a significant reduction in the number of motor neurons and in the area of the spinal cord in mSod1 zebrafish compared to wtSod1

and Ctrl fish. Furthermore, it shows a significant reduction of the white muscle fiber caliber in the corresponding segments of the body wall, particularly severe in the most caudal portion of the trunk in mSod1 zebrafish respect to Ctrl zebrafish. Immunofluorescence staining with antibodies against synaptic vesicle glycoprotein 2A (SV2A) and fluorophore conjugated α-Bungarotoxin (α-Btx) allowed the visualization of presynaptic vesicle clusters and postsynaptic acetylcholine receptors (AChRs) clusters, respectively, of neuromuscular junctions (NMJs) on white muscle fibers. Twelve months old mSod1 zebrafish present a significant reduction in the degree of innervation of white muscle fibers, particularly, they show a significant reduction in the density of presynaptic vesicle clusters without a significant reduction in AChRs clusterization or changes in the size of both postsynaptic and residual presynaptic clusters. The ultrastructural analyses of adult zebrafish NMJs do not reveal any alteration in the fine structure of remaining presynaptic terminals but, reveal a significant reduction in muscular mitochondria area in mSod1 adult zebrafish.

Immunohistochemical stainings for glial fibrillary acidic protein (Gfap), an astrocyte marker, and for allograft inflammatory factor 1 (Aif1), a microglial marker in the spinal cord and of activated neutrophils and macrophages at the periphery, show the presence of reactive astrogliosis but not of microgliosis in the spinal cord of both mSod1 and wtSod1 zebrafish and highlights a significant enrichment of activated inflammatory cells in the muscles of the trunk of mSod1 zebrafish.

Our data show that adult zebrafish expressing the mutant form of Sod1 recapitulate most of the major hallmarks of ALS: motor impairment, motor neurons loss, spinal cord and muscular atrophy, NMJs loss, astrogliosis in the spinal cord and the presence of activated inflammatory cells in the denervated muscle validating zebrafish as useful model for the study of ALS. We also observed that the zebrafish model overexpressing of the wild-type form of Sod1 develops mild alterations similarly to wtSOD1 overexpressing mice.

Since embryonic and larval zebrafish spinal cord is functionally and anatomically similar to that of mammals, and shares principles of locomotor network organization and development with them, they represent an ideal model for the study of diseases characterized by alterations affecting locomotor system functionality.

Sod1 G93R zebrafish present precocious alterations of the locomotor network

We performed whole-mount fluorescence staining against acetylated tubulin (AcTub), SV2A and AChR to visualize the processes of spinal motor nerves and neuromuscular junctions development at 24, 48 and 96 hours post fertilization (hpf), to asses if mSod1 expression precociously affects motor neurons outgrowth and their capability to establish functional connections with muscles. Our studies show that Sod1 G93R expressing embryos display a significant reduction in the motor axons length and in the unbranched axonal length and show a significant increase in the number of motor nerves axonal branches compared to Ctrl embryos, along the entire trunk already at 24 hpf. We performed a 3D colocalization analysis between pre- and post-synaptic clusters at 48 hpf and 96 hpf to evaluate if mSod1 expression impairs NMJs development. At 48 hpf, mSod1 larvae do not show differences in the density of developing presynaptic vesicle clusters and AChRs postsynaptic clusters, and in the density of pre and postsynaptic superimposing (colocalizing) clusters compared to Ctrl and wtSod1 embryos. However, we measured a significant increase in the dimension of synaptic vesicle clusters in mSod1 embryos compared to Ctrl and wtSod1, without alterations in the dimension of AChRs clusters. At 96 hpf, this precocious impairment in neuromuscular contacts maturation gets worse, in fact, while the dimension of synaptic vesicles and AChRs clusters result similar among transgenic and non-transgenic larvae, we measured a significant reduction in the density of presynaptic clusters in mSod1 larvae musculature compared to both Ctrl and wtSod1 larvae without alterations in the density of AChRs postsynaptic clusters. Moreover, in mSod1 larvae, we detected also a significant reduction in the association of presynaptic and postsynaptic clusters compared to both wtSod1 and Ctrl fish highlighting a severe impairment in neuromuscular junctions maturation at the very early stages of zebrafish development. The ultrastructural analyses, however, do not show alterations in the newly formed NMJs of mSod1 larvae, in fact, we did not measure any differences in NMJs area, density and morphology of synaptic vesicles, and in the number and shape of mitochondria in the presynaptic terminal among larvae of the three genotypes. Furthermore, in mSod1 larvae we observed a significant reduction in muscle fibers caliber and muscular mitochondrial area and a preservation of the ultrastructure of the contractile apparatus similarly to what observed in adults mSod1 fish.

To evaluate if morphological alterations in the developing motor system of zebrafish embryos and larvae were associated to defects in the motor response, we performed behavioral tests with zebrafish at 20 hpf, 48 hpf and 96 hpf. At 20 hpf, zebrafish embryos expressing mutant Sod1 show a significant increase in the frequency of spontaneous coilings, embryonic movements consisting in a full body contraction that brings the tip of the tail to the head and, in particular, a significant increase in the percentage of multiple consecutive tail coilings. Alterations in mSod1 zebrafish motor responses persist at 48 hpf when they display a significant increase in the duration of the touch evoked tail coilings response and a significant decrease in the maximum angle of tail flexion and at 96 hpf when they show a significant increase in the duration and in the distance travelled during the touch evoked swimming response compared to wtSod1 and Ctrl fish.

These results in behavioral tests addressed to the study of spinal neurons electrical properties in zebrafish embryos. At 20 hpf, only four types of spinal neurons are active: three types of interneurons and motor neurons. At this developmental stage, zebrafish offers the unique situation to study the electrical properties of a small subset of spinal neurons synchronized in a spinal network solely by electrical coupling. These neurons undergo to periodic depolarizations that originate from a combination of pacemaker currents and particularly depend upon persistent sodium current (I_{NaP}). To test if at the basis of the abnormal coiling activity there was an alteration in the periodic depolarizations of spinal neurons we used a FRET-based voltage biosensor called Mermaid. This biosensor, expressed under the control of a pan-neuronal specific promoter (HuC), was microinjected into one-cell fertilized zebrafish eggs. In this way we obtained the expression of the biosensor in the plasmamembrane of a limited identifiable subpopulation of neurons and thanks to the measurement of the FRET Ratio we manage to study membrane voltage changes in different neuronal subtypes. We recorded periodic depolarizations in motor neurons and in the active population of interneurons and we detected a significant increase in the frequency of the periodic depolarizations in motor neurons and interneurons of mSod1 embryos compared to those recorded in Control fish, without differences in their amplitude, duration and basal membrane FRET Ratio.

Since it has been demonstrated that, at the basis of periodic depolarizations there is the pacemaker sodium current I_{NaP} and that this current is selectively inhibited by 5 μM concentration of riluzole, we tested whether the increase in periodic depolarization and ultimately, the spontaneous coiling phenotype in mSod1 embryos, were caused by I_{NaP} current. To this aim we measured periodic depolarizations and spontaneous coiling in Ctrl

and mSod1 embryos at 20 hpf before and after the administration of 5 μM riluzole. These experiments show that riluzole treatment affects both spontaneous periodic depolarization and coiling activity; in fact, it reduces the frequency of periodic depolarization and spontaneous coiling not only in control embryos but also in those expressing the mutant form of Sod1 bringing them to values comparable to those of Ctrl fish before riluzole administration.

Our results suggest that mSod1 expression, in the zebrafish model, is associated to precocious impairments in neuromuscular junctions maturation and alterations in spinal neurons electrical properties. Spinal neurons hyperexcitability is associated to I_{NaP} current altered activity that also causes aberrant spontaneous coiling behavior in mSod1 embryos. Furthermore we demonstrated the possibility to pharmacologically modify spinal neurons electrical activity and the behavioral phenotype by administering riluzole directly into the embryo water.

Our study reveals that the Sod1 G93R zebrafish model represents a very powerful tool in ALS research.

Adult zebrafish expressing mutant Sod1 develop most of the main pathological features occurring in ALS that have already been well identified and documented in humans and other animal models of the disease.

Mutant embryos and larvae show easily detectable precocious morphological alterations affecting the locomotor network: defective motor nerves outgrowth and neuromuscular junctions maturation, impairment that could be used to set up high-throughput drugs screening platforms to identify potential drugs for ALS treatment. Moreover, they represent a unique system to investigate the role of neuronal hyperexcitability in an intact developing neuronal network, taking advantage of the unique condition of exclusive electrical coupling among neurons in such a precocious form of spinal locomotor circuit

INTRODUCTION

1. AMYOTROPHIC LATERAL SCLEROSIS

Amyotrophic lateral sclerosis (ALS), also known as Lou Gehrig's disease, is a fatal, highly debilitating disease caused by the progressive degeneration of lower motor neurons in the brainstem and spinal cord and of upper motor neurons in the motor cortex. The term "amyotrophic" refers to the muscle atrophy, weakness and fasciculations that indicate disease of the lower motor neurons, while "lateral sclerosis" refers to the hardening of lateral columns, where gliosis follows the degeneration of corticospinal tracts.

First described in 1869 by the French neurologist Jean-Martin Charcot, ALS belongs to the group of disorders classified as motor neuron diseases (MNDs) and is the most frequent adult-onset motor neuron disorder.

The annual worldwide incidence of new cases of approximately 1 to 2.5 per 100,000 individuals is fairly uniform, except for a few high-incidence foci, such as the Kii Peninsula in Japan and Guam. The global prevalence of ALS is 3 to 6 per 100,000. The mean age of onset is 55–60 years and the disease more commonly affects men than women.

The progressive failure of the neuromuscular system results in weakness and atrophy of the limb musculature, progressive paralysis and eventually death from respiratory failure typically within 2 to 3 years of symptoms onset, with 7 - 20% of patients surviving for more than 5 years from the time of diagnosis (Renton et al., 2014; Ferraiuolo et al., 2011; Habib & Mitsumotu, 2011).

As of yet, there are no effective cures for ALS, although riluzole (2-amino-6-tri fluoromethoxy benzothiazole, RP-54274, Rilutek^{TM}) the only drug currently approved (by the Food and Drug Administration (FDA) in the United States, by the Committee for Proprietary Medicinal Products (CPMP) in Europe and the Ministry of Health, Labor and Welfare (MHLW) in Japan) for ALS treatment, slows the rate of progression and may prolong survival times by as much as three months (Bensimon et al., 1994; Bellingham, 2011).

1.1 Clinical features and diagnosis

ALS exhibits a diverse and complex clinical phenotype that complicates the understanding of its pathophysiology and makes it difficult to diagnose. The diagnosis of ALS has been standardized by the El Escorial criteria for clinical research, is based on the history and physical examination of patients showing progressive upper and lower motor

neurons dysfunction and is usually supported by electrophysiological and neuroimaging investigations and laboratory tests (Kiernan et al., 2011).

Generally speaking, the disease is characterized by the coexistence of signs of degeneration in the upper and lower motor neurons encompassing the progressive deterioration of multiple body regions. The disease starts with limb weakness in about two-thirds of patients, often preceded by cramps, while in the remaining one-third bulbar weakness begins, eventually causing dysarthria and dysphagia. Although fasciculations are a cardinal feature of ALS, they are not necessarily the presenting symptom.

The characteristic combination of upper and lower motor neuron dysfunction is usually evident on neurological examination: it is characterized by the presence of weakness, atrophy and fasciculations together with hyperreflexia and increased tone in the same motor segment and, frequently, an extensor response to plantar stimulation (Babinski sign). The disease spreads contiguously to other parts of the body, generally sparing sensory functions. In many patients the disease begins with limb-onset typically associated with preferential wasting and weakness of the thenar muscles. In other cases, bulbar-onset symptoms include flaccid or spastic dysarthria, dysphagia, hoarseness, tongue wasting, weakness, and fasciculations, as well as emotional lability and pathological brisk jaw reflexes. In addition, subtle cognitive abnormalities such as executive dysfunction, language and memory impairment, together with behavioral abnormalities may be evident in up to 50% of ALS patients and may precede the onset of motor symptoms. Dysphagia may result in aspiration pneumonia, malnutrition, and weight loss, leading to a more rapid deterioration of afflicted individuals. Eventually, the disease spreads to respiratory muscles leading to death from respiratory failure within 30 months on the average. Respiratory dysfunction, although in some aggressive cases could be the presenting symptom, usually develops in the latter advanced stages of ALS, ultimately resulting in terminal respiratory failure and death (Vucic et al., 2014 and references therein; Ajroud-Driss & Siddique, 2014).

1.2 Pathological changes

Peculiar gross and microscopic pathological changes, beside specific clinical symptoms, characterize the disease. Individuals affected by ALS show gross anatomical changes: like atrophy of the precentral gyrus, shrinkage, sclerosis and pallor of the corticospinal tracts, thinning of the spinal ventral roots and hypoglossal nerves, and

atrophy of the somatic and bulbar muscles.

Typical microscopic changes can be observed in the depletion of about 50% of the spinal cord motor neurons, atrophy and basophilic changes in surviving motor neurons, presence in surviving lower motor neurons of ubiquitinated inclusion bodies, depletion of giant pyramidal neurons (Betz cells) in the motor cortex, diffusion of astrocytic gliosis in spinal gray matter and in the gray matter of the motor cortex and in the underlying subcortical white matter, evidence of microglial activation in pathologically affected areas and cytoplasmic aggregate inclusions within glial cells (Ferraiuolo et al., 2011).

1.3 Pathogenetic mechanisms

The pathogenic processes underlying ALS are multi-factorial and not fully understood (Vucic et al., 2014). Newly identified genes associated with ALS suggest that, at the base of the pathology, a complex interplay between multiple mechanisms exists, including: genetic factors, impairments in RNA processing and axonal transport, mitochondrial dysfunction, protein aggregation, excitotoxicity and oxidative stress (Figure 1).

Figure 1

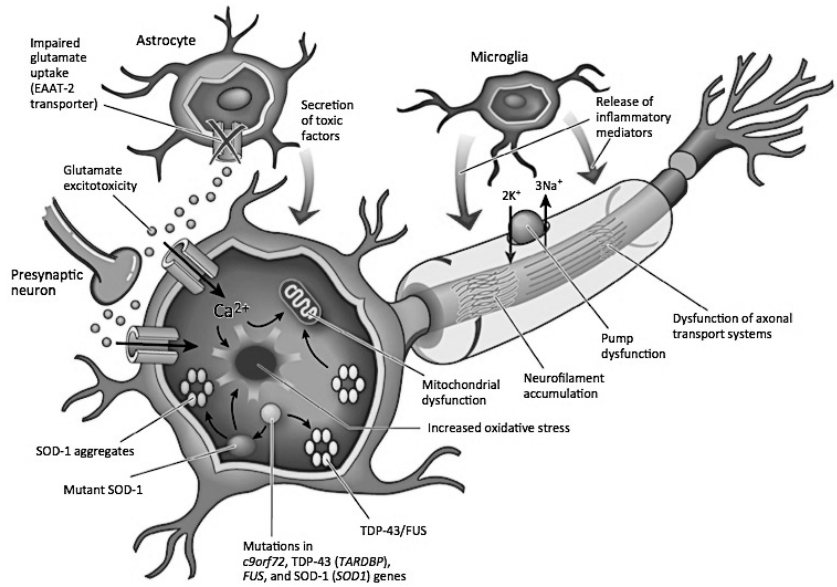

Figure 1: Pathogenetic mechanisms of ALS. Motor neuron degeneration in ALS results from a complex interplay between molecular and genetic pathways. Mutations in C9orf72, TDP-43 and FUS cause the deregulation in RNA metabolism leading to the formation of harmful intracellular aggregates. Astrocytic excitatory amino acid transporter 2 (EAAT2) dysfunction causes the reduction of glutamate uptake from the synaptic cleft and glutamate-induced excitotoxicity that causes an increase of Na^+ and Ca^{2+} ions influx and ultimately neurodegeneration through activation of Ca^{2+}-dependent enzymatic pathways. Mutant SOD1 enzymes increase oxidative stress, induce mitochondrial dysfunction, form intracellular aggregates and adversely affect neurofilament and axonal transport processes. Microglial activation results in proinflammatory cytokines secretion contributing to further toxicity (modified from Vucic et al., 2014).

1.4 Genetic factors

The majority of ALS cases, about 90%, occurs randomly throughout the population and is termed sporadic (SALS), while about 10% of ALS cases have a family history of the disease and are classified as familial (FALS). From the clinical point of view, FALS and SALS are indistinguishable, however, patients with familial disease may be younger at onset. Moreover, while men have a higher incidence of sporadic disease, in FALS, caused by genes with autosomal dominant inheritance, men and women are equally affected (Habib & Mitsumotu, 2011).

A genetic etiology has been identified in up to 20% of apparently sporadic ALS cases and 60% of familial ALS cases, with at least 21 genes and genetic loci being implicated in ALS pathogenesis, usually of autosomal dominant inheritance (Figure 2) (Renton et al., 2104). Although the mechanisms underlying ALS pathogenesis remain elusive, the progress made in unraveling the genetic etiology of ALS has provided fundamental insights into the cellular mechanisms underlying neuron degeneration, not only in the minority of cases that carry familial ALS mutations, but also in sporadic ALS cases.

Figure 2

Table 1 Genes known to carry ALS-causing mutations

Gene	Location	Inheritance	Percentage explained		Putative protein function
			Familial ALS	Sporadic ALS	
TARDBP	1p36	AD	4	1	RNA metabolism
SQSTM1	5q35	AD	1	<1	Ubiquitination; autophagy
C9ORF72	9p21	AD	40	7	DENN protein
VCP	9p13	AD	1	1	Proteasome; vesicle trafficking
OPTN	10p13	AR and AD	<1	<1	Vesicle trafficking
FUS	16p11	AD and AR	4	1	RNA metabolism
PFN1	17p13	AD	<1	<1	Cytoskeletal dynamics
SOD1	21q22	AD and AR	12	1–2	Superoxide metabolism
UBQLN2	Xp11	XD	<1	<1	Proteasome

Table 2 Other genes implicated in the pathogenesis of ALS

Gene	Location	Inheritance	Predominant clinical syndromes	Putative protein function
DCTN1	2p13	AD	PMA; Perry syndrome	Axonal transport
ALS2	2q33	AR	Juvenile PLS; infantile HSP	Vesicle trafficking
CHMP2B	3p11	AD	Familial ALS; sporadic ALS; FTD	Vesicle trafficking
FIG4	6q21	AD and AR	CMT; familial ALS	Vesicle trafficking
HNRNPA2B1	7p15	AD	Multisystem proteinopathy; ALS	RNA metabolism
ELP3	8p21	Undefined	Sporadic ALS	RNA metabolism
SETX	9q34	AD	Juvenile ALS; ataxia with oculomotor apraxia	RNA metabolism
HNRNPA1	12q13	AD	Multisystem proteinopathy; ALS	RNA metabolism
ATXN2	12q24	Undefined	Sporadic ALS; ataxia	Endocytosis; RNA translation
ANG	14q11	AD	Familial ALS; sporadic ALS	Angiogenesis
SPG11	15q14	AR	Juvenile ALS; HSP	DNA damage repair
VAPB	20q13	AD	PMA; FALS	Vesicle trafficking
NEFH	22q12	AD	Familial ALS; sporadic ALS	Axonal transport

Figure 2: Genes carrying ALS-causing mutations and genes implicated in ALS pathogenesis. Values represent the percentage of ALS explained by each gene in population of European ancestry. Abbreviations are: AR, autosomal recessive; AD, autosomal dominant; XD, X-linked dominant; DENN, differentially expressed in normal and neoplasia; CMT, Charcot-Marie-Tooth disease; HSP, hereditary spastic paraplegia; PLS, primary lateral sclerosis; PMA, progressive muscular atrophy (modified from Renton et al., 2014).

1.5 Deregulated transcription and RNA processing

One of the most recent and important advances in unraveling the genetic etiology of ALS occurred with the discovery of the dominantly inherited C9orf72 gene expansion, which appears to underlie more than 40% of familial and 20% of sporadic ALS cases (Renton et al., 2011). This monumental discovery has radically altered the understanding of ALS pathogenesis, implying that ALS is a multisystem neurodegenerative disorder rather than a pure neuromuscular disease.

In 2011 Renton and colleagues demonstrated that a large intronic repeat expansion (increased GGGGCC hexanucleotide repeat expansion) has been implicated in ALS; however, the precise mechanism by which the C9orf72 gene expansion leads to neurodegeneration in ALS, is not fully comprehended. Given that repeat expansions are known to disrupt RNA metabolism in other neurodegenerative diseases, the involvement of disrupted RNA metabolism in the occurrence of ALS seems to be important in the survival of motor and frontal cortex neurons.

The potential pathogenic mechanism proposed for this mutation is gene haploinsufficiency because it has been reported a reduction in the levels of both short and long isoforms of C9orf72 mRNA in ALS patients (Renton et al., 2011; Ciura et al., 2013). Moreover, blocking the translation of the zebrafish *c9orf72* orthologue using antisense morpholinos results in motor neurons axonal defects in 48 hpf zebrafish larvae and locomotion deficits (Ciura et al., 2013). The second mechanism proposed for the C9orf72 repeat expansion is RNA-mediated toxicity. Intranuclear RNA foci containing C9orf72 hexanucleotide repeats and specific RNA-binding proteins associated with the C9orf72 expansion have been identified as causing the formation of intranuclear and cytoplasmic inclusions and the formation of r(GGGGCC) RNA G-quadruplex structures, that could sequester transcription factors like ASF/SF2 and HNRNPA1, that are crucial in DNA/RNA metabolism, with a toxic effect on cells survival (Mori et al., 2013).

The crucial role of DNA/RNA metabolism in causing ALS is further supported by the identification of mutations in transactive-region DNA-binding protein gene (TARDBP) and fused in sarcoma (FUS) that encode DNA/RNA processing peptides. Mutations in TARDBP and FUS proteins represent 4–6% of familial and 0.7–2% of sporadic ALS; to date, approximately 50 mutations have been identified in each protein, and most mutations are dominantly inherited (Andersen & Al-Chalabi, 2011).

TDP-43/TARDBP and FUS are ubiquitously expressed as RNA-DNA binding proteins involved in DNA repair, regulation of RNA transport, translation, splicing, microRNA biogenesis, and the formation of stress granules (Ling et al., 2013). In both cases, the expression of mutant TDP-43 and FUS in cultured cells and pathological brain and spinal cord tissues leads to a predominant cytoplasmatic localization of the protein, particularly in cytoplasmic stress granules, both in neuronal and glial cells. Whether motor neuron injury is caused by loss of normal nuclear functions of TDP-43 and FUS in RNA processing, or by toxic gains of function, or both is unknown. TDP-43 and FUS contain two RNA recognition domains, structures that are common to many RNA-interacting proteins, including those that are involved in mRNA transport. TDP-43 and FUS may form part of such RNA transport complexes and, when mutated, could thereby contribute to motor neuron injury through loss of axonal mRNA transport (Mackenzie et al., 2010). The recent discovery that the TDP-43 interactor Matrin 3 (MTR3), a nuclear matrix protein that binds DNA and RNA, is mutated in FALS, further support the crucial role of RNA processing disruption in the disease pathogenesis (Johnson et al., 2014).

Further evidence of dysfunctional RNA metabolism in ALS emerges from the presence of mutations in angiogenin (ANG) and the DNA–RNA helicase senataxin (SETX). Angiogenin, whose expression is increased during hypoxia to promote angiogenesis, acts as a transfer RNA-specific ribonuclease and regulates ribosomal RNA transcription. Senataxin is a component of large ribonucleoprotein complexes, with roles in maintaining DNA repair in response to oxidative stress, and RNA processing (Ferraiulo et al., 2011 and references therein).

1.6 Impaired endosomal trafficking and axonal transport

The dysregulation of the endosomal network, the system at the basis of the delivery of cargoes to their specific destination via a complex system of organelles, and endocytosis, the process by which extracellular molecules are captured at the cell surface membrane and taken into the cell, are crucial cellular mechanisms underlying motor neuron degeneration, that have been implicated in several genetic subtypes of ALS (Ajroud-Driss & Siddique, 2014).

Mutations in Alsin, a guanine nucleotide exchange factor for the small GTPase protein Rab5, involved in endosomal fusion and trafficking, as well as neurites outgrowth, are associated with a form of autosomal recessive juvenile-onset ALS. In neurons, loss of

Alsin function alters AMPAR trafficking and reduces AMPAR subunit 2 (GluR2) at the synapse and at the cell surface (Lai et al., 2006). Also mutations in Vesicle-associated membrane protein-Associated Protein B (VAPB), Optineurin (OPTN): a component of the endosomal sorting complex required for transport (ESCRT-III), Charged multivesicular protein 2B (CHMP2B), Valosin-containing protein (VCP) which forms a complex with the endocytotic protein clathrin and the Polyphosphoinositide phosphatase (FIG4), seem to disrupt the endosomal network. This disruption is particularly toxic for motor neurons because of their high demand for a continuous turnover of the membrane components of their long axonal processes (Ferraiuolo et al, 2011 and references therein).

Axonal pathology is another key feature of ALS, and might therefore play a crucial role in the pathophysiology of the disease. Motor neurons are highly polarized cells with long axons, and axonal transport is required for the delivery of essential components (RNA, proteins and organelles) to the axonal compartment, which includes synaptic structures at the neuromuscular junction (NMJ). The principal machinery for axonal transport uses microtubule-dependent kinesin and cytoplasmic dynein molecular motors, which mediate transport towards the NMJ (anterograde transport) and towards the cell body (retrograde transport), respectively. In mSOD1 mice, defective axonal transport occurs early in the disease process; supporting the hypothesis that deregulation of axonal transport plays a part in the pathophysiology of ALS. Mutant SOD1 impairs both anterograde and retrograde transport of several cargoes and the defects seem to be cargo-specific, as only anterograde transport of mitochondria is disrupted. The decreased axonal mitochondrial transport, in turn, could result in defective transport of other cargoes because of the lack of energy required for axonal transport (De Vos et al., 2007). Axonal transport defects are likely to contribute to the “dying-back” process, and in particular defects in anterograde axonal transport and mitochondrial dysfunction may combine to cause energy depletion specifically in the distal axon, ultimately resulting in motor neuron degeneration typical of ALS (Kiernan et al., 2011).

The role of cytoskeletal defects in ALS has been recently emphasized by the discovery of TUBA4A mutations in familial ALS. The pathology associated variants discovered, proved to be inefficient in the formation of α-/β-tubulin dimers *in vitro* and their incorporation into microtubules was decreased in cultured cells; moreover, they inhibited microtubule assembly and reduced microtubule network structural stability probably through a dominant negative mechanism (Smith et al., 2014).

1.7 Excitotoxicity

Glutamate-mediated excitotoxicity is a crucial pathogenetic process, found in both animal and human studies, occurring in familial and sporadic forms of ALS. Glutamate is the main excitatory neurotransmitter in the central nervous system (CNS) and exerts its effects through an array of ionotropic (including N-methyl-D-aspartate (NMDA) and α-amino-3-hydroxy-5-methyl-4-isoxazoleproprionic acid (AMPA) receptors) and metabotropic postsynaptic receptors. The removal of glutamate from the synaptic cleft by glutamate reuptake transporters, the most abundant of which is the astrocytic excitatory amino acid transporter 2 (EAAT2; also known as SLC1A2 or GLT1 in rodents), is fundamental in the termination of the excitatory signal. The excitotoxicity, that is the neuronal injury resulting from excessive activation of glutamate receptors, may be caused either by increased synaptic levels of glutamate or by the higher sensitivity of the postsynaptic neuron to glutamate. It could be due to alterations in neuronal energy homeostasis or glutamate receptors expression. This phenomenon causes an increase of Na^+ and Ca^{2+} ions influx leading to: the disruption of intracellular calcium homeostasis, the activation of Ca^{2+}-dependent proteolytic enzymes and ROS-generating enzymes, the perturbation of mitochondrial function and ATP production and, ultimately, neurodegeneration (Vucic et al., 2014; Ferraiuolo et al., 2011).

Evidence from neural cultures seem to highlight that motor neurons are especially vulnerable to AMPAR-mediated excitotoxicity; in fact, motor neurons express lower levels of GluR2 AMPAR subunit in comparison with other subunits and respect to other neuronal cell types. This subunit determines the calcium permeability of the AMPAR complex because, thanks to its post-transcriptional editing at the Gln/Arg site 586 in the second transmembrane domain, it contributes to the Ca^{2+} impermeability of the receptor complex (Williams et al., 1997). ALS patients showed specific GluR2 AMPAR subunits editing defects and reduced expression of proteins with Ca^{2+}-buffering capacity; both mechanisms increase motor neurons vulnerability to degeneration and susceptibility to glutamate excitotoxicity (Van Damme et al., 2005). Moreover, in some patients with ALS, the glutamate levels in the cerebrospinal fluid are more elevated than either in healthy subjects or subjects affected by other neurological diseases (Shaw et al., 1995). A lower expression and reduction in the high-affinity sodium-dependent glutamate transport were identified in synaptosomes obtained from motor cortex and spinal cord of ALS patients (Rothstein et al., 1992). In addition, the overexpression of the astrocytic glutamate

transporter EAAT2 was demonstrated to be neuroprotective (Guo et al., 2003), whereas downregulation of EAAT2 accelerated disease progression (Pardo et al., 2006) in ALS mouse models.

1.8 Oxidative stress

Reactive oxygen species (ROS) such as superoxide anion (O^{2-}) and hydrogen peroxide (H_2O_2) are products of normal oxygen metabolism in cells. They serve as signaling molecules but, when present in excess, can alter the structure and functions of the cell (Vehviläinen et al., 2014). Oxidative stress arises from an imbalance between the generation and removal of reactive oxygen species and/or from a reduction in the ability of the biological system to remove or repair ROS-induced damage. The accumulation of oxidative stress in non-replicating neurons during the aging process due to the presence of a disease-causing mutation in a protein involved in the protection from toxic insult could culminate in neuronal death and onset of neurodegeneration in middle or later life.

The role of oxidative stress in ALS pathogenesis became of particular interest after the identification of ALS associated mutation in the protein Cu-Zn Superoxide Dismutase (SOD1): a major antioxidant protein (Rosen et al., 1993).

Since most information regarding ALS pathogenetic mechanisms and pathophysiology have been collected through the study of animal models carrying mutated forms of SOD1; in the following sections, we will expand our discussion of the typical phenotype of ALS in humans and animal models associated to SOD1 mutations.

2. THE DISCOVERY OF CU-ZN SUPEROXIDE DISMUTASE 1 MUTATIONS: A MILESTONE IN THE STUDY OF ALS PATHOLOGY

In 1993, a landmark discovery of 11 missense mutations in the SOD1 gene, in 13 FALS families (Rosen et al., 1993), heralded the genetic age for ALS.

2.1 Copper-Zinc Superoxide Dismutase 1

SOD1 is a ubiquitously expressed homodimeric metalloenzyme of 153 amino acids with a stabilizing zinc ion and two catalytic copper ions in each subunit. The two subunits are tightly packed and held together by strong hydrophobic interactions between the β-strands, making the dimer extremely stable (Figure 3). Mainly enriched in the cytoplasm, it localizes also in the mitochondrial intermembrane space and in the nucleus. Both, in the cytoplasm and in the intermembrane space, SOD1 functions by detoxifying intracellular superoxide anions (O^{2-}) catalyzing the dismutation of superoxide anion radical to molecular oxygen (O_2) and hydrogen peroxide (H_2O_2) that is further reduced to water (H_2O) by catalase, glutathione peroxidases or peroxiredoxins. SOD1 is found in all cells in almost all organisms above the bacteria and the aminoacidic sequence is evolutionarily highly conserved, suggesting that SOD1 plays a crucial function in cellular homeostasis (Andersen, 2006).

Figure 3

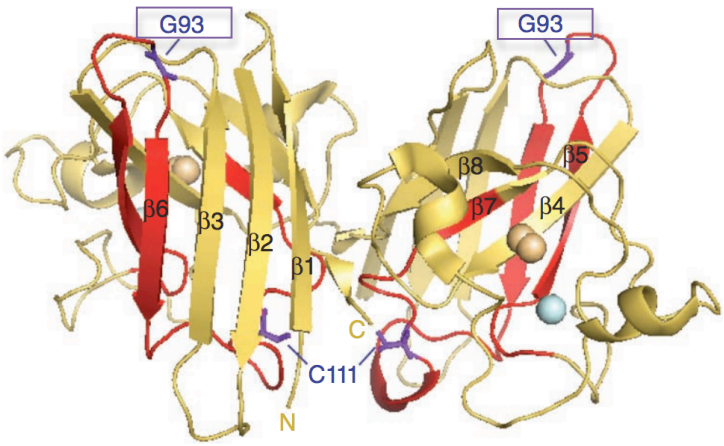

Figure 3: Structure of wild-type SOD1.
X-ray crystallographic structure of wild-type SOD1. The zinc and copper atoms are shown in cyan and orange, respectively. Wild-type SOD1 residues G93 in exon 2 are highlighted and labeled in purple (modified from Bosco et al., 2010).

The SOD1 gene is a small gene of five exons separated by four introns positioned on chromosome 21. To date 166 SOD1 mutations have been reported, underlying 14–23% of familial and 1–7% of sporadic ALS cases (Vucic et al., 2014).

The mutations discovered encompass all coding regions of the gene with preponderance for exons 4 and 5. Only few mutations have been found in the 24 codons of exon 3 that encode the amino acids forming the catalytic site and the zinc loop. Interestingly, no mutations have been identified between Q22 and G37 in exons 1 and 2, all truncating mutations lie in exons 4 and 5 and no null mutations have been found suggesting that at least the amino terminus of the SOD1 polypeptide is essential for the cytotoxic effect. Moreover, glycine-93 appears particularly vulnerable, since it is point mutated to all 6 possible residues in FALS. The mutations include missense, nonsense, sense and in-frame deletions in the coding sequence but also mutations occurring in noncoding sequence predicting aberrant mRNA splicing (Andersen, 2006). Thus, the majority of SOD1 mutations encode polypeptides with single amino acid substitutions and a subset with C-terminal truncation (Orrell et al., 1999). All SOD1 mutations associate with dominant ALS, with the exception of N86S and D90A substitutions, which behave as recessive traits (Turner & Talbot, 2008). The D90A mutation is the globally most frequent SOD1 mutation also in the sporadic population. It has been found in most European countries, North America and Russia and it is present in 0.5% to 5% of healthy population, usually in heterozygous form, in the Kola Peninsula in Finland, northern Sweden and Norway. This substitution correlates with a non-penetrant or slowly progressive disease. The A4V mutation is the second most frequent mutation. Widely spread in the United States, it is associated with a dramatic phenotype with sudden low motor neurons signs in the limbs, trunk or bulbar innervated muscles leading to dead in 1 to 2 years after diagnosis (Andersen, 2006).

Most SOD1 mutations are characterized by intra- and interfamilial variability in penetrance, age and site of disease onset, rate of disease progression, and survival, with approximately 50% of patients expressing the disease by age 43 and more than 90% by 70 years (Vucic et al., 2014; Orrell et al., 1999).

In the genetic subgroup of ALS associated with SOD1 mutations, the common clinical features are asymmetrical onset distally in a limb (usually a leg), proximal onset in the pelvic-girdle musculature or in the upper limbs and rarely a bulbar onset. A common denominator for all mutations is the predominance of lower motor neurons features (Orrell et al., 1999), but upper motor neurons manifestations may be present. For several

mutations non-motor signs have been also reported (Andersen, 2006).

2.2 Pathogenetic mechanisms associated with SOD1

The pathophysiological mechanisms by which SOD1 gene mutations lead to neurodegeneration are still unclear. SOD1 mutations that cause amino acid substitutions at metal-binding ligands (H46R, H48Q, H48R, and H80R) or at residues in the electrostatic loop (S134N and D125H) might affect protein metal-binding affinity or enzymatic activity. Likewise, mutations at the disulfide bond (C146R) or at residues near the dimer interface (V148G, I149T, A4V, and I113T) might be expected to influence the protein stability and structure (further considering that C-terminal truncations remove substantial portions of the protein involved in catalysis, metal binding, and dimerization). Ultimately, SOD1 mutations can be partitioned into two groups with distinctly different biophysical characteristics with respect to metal content, SOD activity, and spectroscopy: the metal-binding region (MBR) and the wild-type-like (WTL) FALS mutant SOD1. The MBR subset of SOD1 proteins have mutations that are localized in and around the metal-binding sites, including the electrostatic and zinc loops, and were found to have a significant reduction in the enzymatic activity in comparison with wild-type SOD1; while, the WTL subset of SOD1 proteins was found to be remarkably similar to wild-type SOD1 in most of their properties (Valentine et al., 2005).

Since the lack of SOD1 does not lead to the development of ALS in mice (Reaume et al., 1996) and SOD1 mutations causing ALS are associated either with a wild-type-like or a markedly reduced enzymatic activity (Valentine et al., 2005); it has been suggested that the potential pathogenetic mechanisms are those mediated by a specific protein cytotoxicity (Vehviläinen et al., 2014; Turner & Talbot, 2008) or protein aggregation (Durazo et al., 2009; Bosco et al., 2010). The first toxic mechanism proposed is that mediated by the increased production of hydroxyl and free radicals (Vehviläinen et al., 2014), as well as nitration of tyrosine residues on proteins (Turner & Talbot, 2008). Evidence for oxidative damage has been inferred from pathological studies in ALS patients and transgenic SOD1 mouse models (Turner & Talbot 2008 and references therein). Although oxidative damage seems to be an attractive pathogenic mechanism, findings of normal SOD1 activity in patients harboring particular SOD1 mutations, the absence of correlation between dismutase activity and disease severity and the lack of beneficial effects of anti-oxidants in ALS patients all suggest a minor role for oxidative stress in SOD1-related ALS pathogenesis (Vucic et al., 2014 and references therein). The second

pathogenetic mechanism proposed is that due to the conformational instability of the mutated SOD1 peptide, resulting in the formation of intracellular aggregates (Durazo et al., 2009; Bosco et al., 2010); in fact, the severity of the disease in patients with SOD1 mutations appears to be correlated with the instability of the mutant SOD1 protein (Valentine et al., 2005; Andersen, 2006). Also in this case, the way by which conformational changes in SOD1 protein lead to neurodegeneration remain to be determined, although co-aggregation of essential cellular components or induction of aberrant catalysis by misfolded SOD1 mutant proteins have been proposed as potential toxic processes (Vucic et al., 2014 and references therein; Turner & Talbot 2008; Valentine et al., 2005).

All these hypotheses are further complicated by the findings that mutant SOD1 mediated toxicity is non-cell autonomous, because lower motor neurons degeneration requires the expression of mutant SOD1 protein within other types of spinal cord cells (Pramatarova et al., 2001; Lino et al., 2002; Clement et al., 2003).

2.3 Transgenic animal models expressing mutant SOD1

For human neurodegenerative diseases, like ALS, human pathologists completely depend on human autopsy samples to gain information regarding the etiology and pathogenesis of motor neurons death. Since it is impossible to safely and repeatedly remove tissues for analyses from patients in real time, and almost all ALS autopsy samples are obtained from affected individuals at the terminal stage, it is difficult to clarify how, why and when ALS motor neurons are damaged in each clinical stage from disease onset to death studying pathology exclusively in humans. Moreover, analyses of ALS autopsy samples alone cannot contribute to the development of possible therapies for the disease. Given all these reasons, the ability to study cellular and molecular processes, identify key pathways for intervention, and assess multiple candidate therapies over short periods of time, depends on the development of disease animal models (Kato, 2008).

Mouse models

Most of our current knowledge of ALS pathogenic mechanisms comes from transgenic mice expressing various forms of mutant SOD1. The proof that SOD1 mutations cause ALS is based on the generation of transgenic mice models, expressing mutant SOD1, capable to recapitulate the disease. To date, studies with these animals

highlighted most of the targets of damage in the disease (Turner & Talbot, 2008 and references therein).

SOD1 knockout mice allowed to exclude that the disease was due to SOD1 loss-of function. Although the global distribution of SOD1 mutations across all exons intuitively suggested a loss-of-function mechanism at the basis of ALS pathogenesis and early observations of reduced dismutase activity in erythrocytes of patients heterozygous for SOD1 mutations led to support this hypothesis; mice deficient for SOD1, generated by targeted gene deletion, were viable and appeared to develop without obvious motor abnormalities (Reaume et al., 1996).

Transgenic lines overexpressing the wild-type form of SOD1 were also generated. Although these aged animals undergo to subclinical motor neurons degeneration, hypotonia, hind limb neuromuscular pathology, vacuolar pathology and axonal loss (Dal Canto & Gurney, 1995) no lines of transgenic wild type SOD1 mice have succumbed to ALS symptoms to date (Turner & Talbot, 2008).

The discovery of SOD1 mutations in FALS was promptly followed by the generation of transgenic mice constitutively expressing mutant SOD1. These animals were generated with vectors containing 12–15 kb of human genomic fragments encoding SOD1 driven by the endogenous promoter and regulatory sequences. The first animal model that recapitulated many of the ALS-like phenotypes was created expressing the human SOD1 gene, encoding a mutation found in FALS cases that converts glycine residue 93 to an alanine (G93A) in mouse under the control of the human SOD1 promoter (Gurney et al. 1994). Subsequently several other models have been generated: 12 different SOD1 human ALS mutations, as well as artificially induced SOD1 mutant transgenes that either prevent copper binding (H46R/H48Q and H46R/H48Q/H63G/H120G) or truncate SOD1 protein at threonine residue 116 (T116X) have been expressed in the mouse. Interestingly, the transgenic expression of a mutated mouse Sod1 G86R transgene also causes ALS-like phenotypes in mice. Despite vast differences in transgene copy number, steady-state transcript and protein levels, dismutase activity and neuropathology, the mutations induce fatal symptoms strongly indicative of ALS with different disease latencies and progression rates. Crucially, the disease phenotype of transgenic mice expressing SOD1 mutants on a background of endogenous enzyme argued for a dominant gain-of-function mechanism in toxicity (Joyce et al., 2011; Turner & Talbot 2008).

In most cases, mice overexpressing the wild-type form SOD1 are used as a control model for mutant SOD1 transgenic models since they overexpress exogenous protein and

do not develop overt motor phenotypes; however, as it was described before, it is important to highlight that these mice exhibit a subclinical neuromuscular pathology, suggesting that SOD1 overexpression causes neuronal defects even without a pathogenic mutation (Rotunno & Bosco 2013; Jaarsma, 2006).

Rat models

Although most of the work on rodents has been focused on SOD1 transgenic mice, two human SOD1 mutations are modeled in rats: SOD1 H46R and SOD1 G93A. Similarly to mice, these transgenic animals have progressive degeneration of both upper and lower motor neurons and disease severity is directly proportional to mutant SOD1 expression levels. The SOD1 G93A mutation causes a more aggressive disease in rats than the SOD1 H46R mutation, and differently from mouse models, onset of muscle weakness occurs in either the forelimbs or the hind limbs. These rat models offer the advantage of increased size of organs and tissues, facilitating surgical interventions and preclinical trials (Joyce et al., 2011).

Dog expressing SOD1 mutation

A SOD1 mutation has been recently identified at the basis of a canine degenerative myelopathy. This mutation consists in the aminoacidic substitution E40K, a change that has also been identified in human ALS cases. The SOD1 E40K mutation identified in dogs is the first example of a spontaneous disease-causing mutation in SOD1 outside of humans. Differently from human patients, where this mutation is transmitted with an autosomal dominant pattern, in the dog is predominantly recessive with incomplete penetrance. The degenerative myelopathy in the dog has a midlife onset, always begins with the loss of upper motor neurons functions showing spastic paralysis and progress to lower motor neurons dysfunction resulting in hind limbs and subsequently forelimbs paralysis. Certain heterozygous animals display a subclinical pathology with appearance of cytoplasmic SOD1 aggregates in the spinal cord. Since SOD1 expression in these animals is at endogenous levels, dogs suffering from this disease present a rare opportunity to study a naturally occurring ALS-like disorder (Joyce et al., 2011 and references therein).

Zebrafish models

Human wild-type SOD1, SOD1 G93A, SOD1 G37R, and SOD1 A4V mRNAs were each injected into zebrafish embryos to study the effects of the transient overexpression of mutant SOD1 in zebrafish. Mutant SOD1, but not wild-type SOD1, caused an axonopathy phenotype 30 hours post-fertilization (hpf) characterized by decreased axonal length and aberrant branching (Kabashi et al., 2011; Lemmens et al., 2007). While these results reflect a toxic effect of mutant ALS proteins on developing motor neurons axons, the transient expression in these models limits the amount of insight that can be gained regarding the mechanisms of progressive neurodegeneration that is characteristic of ALS.

Two stable transgenic zebrafish lines overexpressing mutant zebrafish Sod1 G93R (Ramesh et al., 2010) and human SOD1 G93A (Sakowski et al., 2012) have been generated so far. In both cases, the overexpression of the mutant protein causes slow-progressing ALS-like defects: defective motor performance, motor neurons loss, reduced survival and in the first case increased heat shock stress response in spinal neurons and a reduction in glycine release (McGown et al., 2013). In both models, NMJ defects such as shorter and more punctate NMJ presynaptic boutons have also seen (Ramesh et al., 2010; Sakowski et al., 2012).

Recently, it has been reported the generation of a zebrafish model expressing the mutant zebrafish T70I Sod1 at physiological levels. These fish show an altered NMJ morphology, an increased susceptibility to oxidative stress and an adult onset motor impairment that recapitulated the key features of ALS (Da Costa et al., 2014).

Invertebrate models

Given that many disease genes are conserved across evolution, invertebrate organisms can be an ideal system to investigate, at the cellular level, not only pathogenic mechanisms linked to causative mutations, but also to uncover potential genetic interactions that may point to new therapeutic targets among these genes (Casci & Pandey, 2014; Therrien & Parker, 2014).

In recent years, transgenic *Drosophila melanogaster* overexpressing either *Drosophila* SOD1 (dSOD1), wild-type human SOD1 (hSOD1), or mutant human SOD1 (A4V or G85R) have been generated (Watson et al., 2008). Flies expressing wild-type human SOD1 or either mutant proteins had a reduced climbing ability compared to dSOD1 flies, suggesting a motor neuron dysfunction due to expression of either wild-type or

mutant versions of human SOD1. The differences in climbing did not become apparent until day 14, an observation that suggests a progressive loss of motor function in the wild-type and mutant human SOD1 expressing flies. In addition, these flies exhibited reduced synaptic transmission in dorsal longitudinal muscles of the giant fiber motor pathway and, consistently with SOD1-associated ALS pathogenesis in mouse models, the motor neurons developed aggregates of human SOD1 proteins (Watson et al., 2008). The ubiquitous expression of a zinc-deficient human SOD1 (harboring the D83S mutation in the zinc-binding domain) led to age-dependent locomotor dysfunction, a sever alteration in muscular mitochondria ultrastructure and a decreased ATP production in the brain not present in control flies; even though these flies exhibited normal lifespans and showed no brain degeneration (Bahadorani et al., 2013). Since ALS is thought to be a non-cell autonomous neurodegenerative disease non-neuronal cells have been studied also in *Drosophila* models of ALS. Interestingly, it has been demonstrated that a severe impairment in climbing activity at 60 days occurs in flies expressing wild-type and mutated human SOD1 A4V or SOD1 G85R only in glial cells (Islam et al., 2012).

Several groups have used *Caenorhabditis elegans* to model SOD1 toxicity. The ubiquitous expression of human mutant SOD1 A4V, G37R and G93A impairs the worm's response to oxidative stress and causes protein aggregates (Oeda et al., 2001). The expression of human mutant SOD1 G85R throughout the worm's entire nervous system resulted in locomotor defects and impaired neuromuscular transmission with the formation of aggregates in certain types of mechanosensory neurons despite the pan neuronal expression of SOD1 (Wang et al., 2009). More recently, a *C. elegans* model expressing human SOD1 G93A in motor neurons was generated; it shows an age-dependent paralysis and neurodegeneration in the absence of caspases, an intriguing finding since the motor neuron loss observed in mouse models is associated with caspase activation. Whether this reflects a difference between invertebrate and vertebrate systems, or reflects a novel mechanism of neurodegeneration remains to be determined (Li et al., 2014).

It is worth noting that both in the case of *D. melanogaster* and *C. elegans* expressing mutant forms of SOD1 they do not display motor neuron loss or reduction in the life span probably because of their short life cycle (Watson et al., 2008; Bahadorani et al., 2013; Therrien & Parker, 2014 and references therein; Casci & Pandey, 2014 and references therein).

3. THE STUDY OF SOD1 MUTANT ANIMAL MODELS GIVES US INSIGHT INTO PATHOLOGICAL EVENTS OCCURING IN ALS

Pathological events occurring in ALS have been mainly characterized in the mutant SOD1 mice models but have similarly recapitulated in other animal models. They involve locomotion, spinal cord, peripheral axons, neuromuscular junctions and muscles.

3.1 Clinical phenotype of mutant SOD1 expressing models

Clinical disease in transgenic mice expressing mutant human SOD1 develops and progress in a stereotypic fashion (Figure 4). The high-expressing SOD1 G93A mutant mice (precisely the G1H line, a line derived from the original G1 line generated by Gurney and colleagues in 1994) are the most frequently used for the study of clinical and pathological endpoints because of their short survival and the strong synchrony of disease among mice from the transgenic line. In this line the first consistent sign of disease is a fine shaking or tremor that occurs in one or more limbs around 80-90 postnatal days. With time, the tremor becomes more pronounced and involves all the limbs. These mice present overactive reflexes when lightly tapped on the knee or ankle. As the disease progresses, proximal muscle weakness with marked atrophy develops, usually more evident in the hind limbs than in the forelimbs. As paresis becomes more pronounced, spasticity and hyperreflexia become less, probably because of increasing weakness. The onset of clinical weakness occurs around 125 days of age. At the end-stage disease, around 130 days, mice are severely paralyzed and lie on their side (Chiu et al., 1995; Turner & Talbot, 2008). Although the timing and severity of clinical disease in multiple lines of mice expressing a particular mutant form of human SOD1 correlates with the type of mutation and transgene copy number, the clinical phenotype develops in a stereotypic fashion (Gurney et al., 1994; Chiu et al., 1995; Pun et al., 2006). Later studies, performed on the same mouse model, identified more precocious indication of locomotor impairment: a decreased performance on the accelerating Rotarod already at day 78 and on the constant Rotarod at 85 postnatal days (Fisher at al., 2004) and a significant reduction in the maximum isometric twitch and tetanic contractile force at P60 (Hegedus et al., 2008). It has also been observed that motor functions deficits begin with the initial denervation, in fact, muscle strength tested with the loaded grid test and treadmill gait was impaired in mutant SOD1 G93A mice around 30-40 post natal days (Vinsant et al., 2014a-b).

Regarding the size of mice expressing mutant SOD1, it has been reported that G1H mutant SOD1 mice show a slowing of growth roughly two weeks preceding the onset of tremor, however their weight is within the normal range for non transgenic littermates up to roughly 75 days and then stabilizes hereafter. Only within the last 2 weeks of their illness they loose up to 10% of their body weight (Chiu et al., 1995; Fischer et al., 2004).

Interestingly, clinical disease in mice is observed only in mice expressing mutant human SOD1 while mice expressing wild-type human SOD1 at comparable levels remain free of clinical disease at 1 year of age (Gurney et a., 1994; Chiu et al., 1995).

Motor impairments have been observed also in zebrafish models: Sod1 G93R expressing fish display endurance impairment at 12 months of age (Ramesh et al., 2010) while SOD1 G93A and Sod1 T70I zebrafish spend more time resting than age-matched control AB zebrafish (Sakowski et al., 2012; Da Costa et al., 2013). *Drosophila* models expressing human mutant SOD1 have a reduced climbing ability (Watson et al., 2008; Bahadorani et al., 2013) and human mutant SOD1 G85R and G93A *C. elegans* models display an age-dependent paralysis (Wang et al., 2009; Li et al., 2014).

3.2 Motor neurons degeneration and spinal cord atrophy

Motor neurons death in the SOD1 G93A mouse model is a late stage event (Figure 4). Chiu and colleagues observed a significant loss of somatic motor neurons from the cervical (C7) and lumbar (L7) segments of the spinal cord by 90 days of age, at the onset of clinical symptoms, in the G1H line. Motor neurons degeneration (not detectable at P69) worsened with age and at disease end-stage, motor neurons loss was up to 50% in the same spinal cord levels. Interestingly, not all cholinergic motor neurons were equally affected; in fact the reduction of cholinergic neurons was restricted to the ventral horn of cervical and lumbar spinal cord while no significant reduction in somatic motor neurons innervating axial muscle located at the thoracic (T1-T2) level was recorded (Chiu et al., 1995). Also Fischer and colleagues detected a significant reduction of large motor neurons only at 100 days, although vacuolation of their cell bodies was already observed at 80 days. By day 80, they observed a marked reduction in the density of intact motor axons in the ventral roots with a progressive increase in the proportion of small regenerating caliber axons at 120 days (Fischer et al., 2004). Vinsant and colleagues studied in detail when the loss of motor neurons innervating tibialis anterior and soleus starts in the third, fourth and fifth lumbar region of the spinal cord (L3-L5) in the same SOD1 G93A mouse model. They

observed that at postnatal day 30 (P30) mutant SOD1 motor neurons have a smaller soma area as compared with those in wild-type animals but no differences where found in the size of both soleus and tibialis anterior motor neurons pool between wild-type and mutant SOD1 spinal cords. At P60, although in the SOD1 G93A mouse spinal cord most motor neurons are healthy, a subset of motor neurons contained numerous cytoplasmic vacuoles without a significant loss in the number of cells also at this age. However, SOD1 G93A mice show a higher percentage of vacuolated motor neurons at P60 and at P75 in the spinal cord. By P115–140, there were few remaining vacuolated motor neurons in mutant mice and the number of surviving motor neurons is significantly reduced by approximately 50%. Taken together, these data indicate that cell death begins between P60 and P75, that is heralded by cytoplasmic vacuolization beginning between P44 and P60 and that the total motor neurons loss by end stage is approximately 50% in lumbar spinal cord of mutant mice (Vinsant et al., 2014b). Ventral roots were counted at P75 and no significant differences in the absolute number of ventral root axons in L3, L4, and L5 spinal cord regions were identified between SOD1 G93A and wild-type mice; however, many axons in the SOD1 G93A mouse exhibited alterations indicative of ongoing or impending demyelination and degeneration (Vinsant et al., 2014b).

Motor neurons loss has been evidenced also in stable transgenic zebrafish models: at the end stage of disease in Sod1 G93R model (Ramesh et al., 2010), at 3 years of age in Sod1 T70I fish (Da Costa et al., 2014) and already at 40 days of age in SOD1 G93A zebrafish (Sakowski et al., 2012).

Although invertebrate models expressing human SOD1 mutations present signs of neurons degeneration, they never display a significant loss of these cells (Therrien & Parker, 2014; Casci & Pandey, 2014).

3.3 Muscle denervation long precedes motor neurons death

Many neuromuscular junctions are lost in tibialis anterior and gastrocnemius muscles in mice expressing high levels of human SOD1 G93A from 47 postnatal days on; before any detectable loss of motor axons in ventral roots exiting the spinal cord and long before any clinical sign of the disease, suggesting that ALS is a “dying-back” axonopathy (Frey et al., 2000; Fischer et al., 2004; Gould et al., 2006; Hegedus et al., 2008). However, great variability in muscle denervation appears in different types of muscles; for instance,

initial denervation of the medial gastrocnemius muscle has been reported already by postnatal day 25 (Gould et al., 2006).

Pun and colleagues elegantly demonstrated that the characteristic pattern of selective denervation in FALS reflects the selective vulnerability of different subtypes of motor neurons. In G93A SOD1 mice hind limb muscles, fast fatigable (FF) motor neurons (specifically innervating type-IIb muscle fibers) disconnect their peripheral synapses at P48-52 and lose their intramuscular nerve branches at P50-55. Fatigue-resistant (FR) motor neurons (specifically innervating type-IIa muscle fibers), innervating the same muscle sub compartment, initially sprout to partially reinnervate muscle fibers but are less and less capable of maintaining additional neuromuscular junctions and prune their intramuscular nerve branches at P80-90; in contrast, slow motor neurons (S) (specifically innervating type-I muscle fibers) compensate efficiently through sprouting and continue to maintain greatly expanded motor units to the time when the mice die (Pun et al., 2006).

Neuromuscular junctions defects and loss have been reported as a precocious event in ALS pathogenesis also in zebrafish models; in fact, they have been observed before evident motor impairments (Sakowski et al., 2012) and as soon as 11 days post fertilization (Ramesh et al. 2010).

Synaptic transmission becomes progressively defective even in flies expressing human mutant SOD1 (Watson et al., 2008) and in SOD1 G85R expressing *C.elegans* where, in synaptic puncta that demarcate neuromuscular junctions, a significant reduction of synaptic vesicles and an alteration of their dynamic behavior were observed (Wang et al., 2009).

3.4 Ultrastructural alterations of nerve terminals

Several studies pointed out that nerve terminals represent one of the primary sites of motor neurons degeneration and therefore a site of precocious damage (Frey et al., 2000; Fischer et al., 2004; Gould et al., 2006; Pun et al., 2006; Hegedus et al., 2008).

Mitochondria represent one of the primary targets of the damage induced by mutant SOD1 expression both in motor neurons somata and proximal neurites (Dal Canto & Gurney, 1995; Cappello et al., 2012; Vinsant et al., 2014a-b). The presence of mitochondrial abnormalities in the cell body of SOD1 G93A mice motor neurons is a very precocious alteration, already observed at P7 that worsens while the disease progress (Vinsant et al., 2014a-b). These alterations mainly consist in cristae swelling or swollen

mitochondria with fragmented cristae and split outer double membranes that can be detected also in motor neurons dendrites (Dal Canto & Gurney, 1995; Vinsant et al., 2014b). In the diaphragm of SOD1 G93A mice at symptoms onset, the majority of presynaptic boutons contained mitochondria similar in dimension and morphology to those of wild-type animals; however, in the 40% of presynaptic terminals all the mitochondria were vacuolated, with a pale, empty matrix, disorganized cristae and with a higher size and circularity index compared to the intact ones (Cappello et al., 2012). In tibialis anterior and soleus, larger and more vacuolated mitochondria were observed in the SOD1 G93A expressing mice already at P30 and P14 suggesting that mitochondrial changes precede the onset of denervation; moreover, in both muscles, the number of mitochondria was reduced in SOD1 G93A mice and at P30, 50% of tibialis anterior neuromuscular junctions have mitochondrial aberrations and degenerative inclusions (Vinsant et al., 2014b).

Several other features of nerve terminals present ultrastructural alterations in mutant SOD1 expressing mice. The quantitative analysis of synaptic vesicles at symptoms onset (P85-95) revealed a significant reduction of the total synaptic vesicle density in the nerve endings of mutant SOD1 G93A expressing mice compared to wild-type one without significant alterations in the diameter and morphology of synaptic vesicles and in their distribution in the presynaptic terminal (Cappello et al., 2012). A significant reduction in the junctional fold length was identified in tibialis anterior of mutant SOD1 expressing mice at P30 compared to wild-type but, in this case, no differences in the vesicle density and in the number of docked vesicles was identified in the presynaptic terminal between wild-type and SOD1 mice. At P53, when denervation is progressing, individual neuromuscular junctions with both normal and abnormal nerve-muscle contacts, including some with an absence of synaptic vesicles were identified (Vinsant et al., 2014b).

Ultrastructural alterations in the ventral nerve cord were also identified in the *C. elegans* model expressing human mutant SOD1 G85R. In 4 days old G85R worms, the number and diameter of neuronal processes (mostly axons) were slightly reduced compared with wild-type animals. These neurons presented a significant reduction in the numbers of organelles, including both mitochondria and vesicles, within them. Electron microscopy studies, after high pressure freezing, showed a reduction of synaptic vesicles, more pronounced in the region closest to the presynaptic density, in mutant worms as compared with wild-type animals, where vesicles were densely packed in the presynaptic region including the active zone and periactive zone (Wang et al., 2009).

3.5 Muscle defects

Skeletal muscle is one of the tissues affected, both in sporadic and familial human ALS, outside the central nervous system. Both patients and mouse models expressing mutant SOD1 present functional aberrations and skeletal muscle pathology (Boyer et al., 2013 and references therein).

Several investigators have reported skeletal muscle dysfunction and motor unit dropout in patients and mice expressing mutant SOD1 long before motor neurons death and the onset of clinical symptoms. Most of them show gross atrophy of the skeletal muscle (Gurney et al., 1994; Chiu et al., 1995; Fischer et al., 2004; Cappello et al., 2012) and mutant SOD1 aggregates have been observed in hind limb skeletal muscles of SOD1 G93A mice at 90 days (Turner et al., 2003). Both in a mouse model of ALS (SOD1 G86R transgenic mouse) and in muscular biopsies of human sporadic ALS it has been evidenced signs of precocious mitochondrial dysfunction consisting in the upregulation of mitochondrial uncoupling proteins, key regulators of mitochondrial functions, the depletion of ATP levels one month before disease onset and the reduction of the respiratory control ratio of isolated mitochondria selectively in the muscle but not in neuronal tissues (Dupuis et al., 2003). Moreover, SOD1 G93A overexpression in skeletal muscle leads to ROS overproduction and to an increase in oxidative damage to cellular macromolecules before motor neurons death and clinical onset (Mahoney et al., 2006).

Fast trunk muscle ultrastructural analyses revealed myofibrillar and mitochondrial degeneration, and extensive collagen deposition in G93R zebrafish model (Ramesh et al., 2010) and the ubiquitous expression of zinc-deficient SOD1 in *Drosophila* deteriorates mitochondrial structure causing cristae rearrangement (Bahadorani et al., 2013).

Recent findings suggest that multiple cells participate in ALS pathogenesis because the restricted overexpression of human FALS-causing mutations (SOD1 G93A, SOD1 G85R and SOD1 G37R) in neurons alone is not sufficient to cause an ALS phenotype (Pramatarova et al., 2001; Lino et al., 2002; Clement et al., 2003). In this context, the role of mutant SOD1 expression in skeletal muscle is still debated. Dobrowolny and colleagues selectively expressed mutant SOD1 G93A in mouse skeletal muscle using the myosin light chain promoter and observed the development of an ALS-like muscle pathology in mice: muscular atrophy, reduced muscle strength, impaired contractility, ultrastructural disorganization of myofibrils and mitochondrial morphological alterations (they appear swollen, abnormally shaped, and larger in size, sometimes containing vacuolizations and

disrupted outer membrane) and dysfunction without triggering the degeneration of motor neurons (Dobrowolny et al., 2008). These findings contrast with a similar study from Wong and Martin, where human wild-type and mutated SOD1 G93A and SOD1 G37R, selectively expressed in skeletal muscle, resulted in pathologic phenotypes, in all the three transgenic animals, both in muscles and motor neurons. Transgenic mice showed limb weakness and paresis with motor deficits; skeletal muscles presented oxidative damage to proteins in the mitochondria enriched fraction, protein nitration, myofiber cells death, neuromuscular junctions defects, signs of distal axonopathy and a significant loss and degeneration of motor neurons in the spinal cord (Wong & Martin, 2010). The reasons for this discrepancy are still unclear, it might be due to the fact that the animals used were of a different age, being significantly younger in the work of Dobrowolny and colleagues (1-4 months old) compared to those used by Wong and Martin (10-15 months). Regardless of this, together these studies provide strong evidence that mutant SOD1 is toxic to skeletal muscle and challenged the accepted dogma that motor neuron degeneration, caused by the overexpression of mutant SOD1, is the principal driver of muscle atrophy, on the contrary, it appears that skeletal muscle may be a precocious and active partner in disease pathogenesis.

3.6 Glial cells in ALS

Studies based on animal models showed that ALS is a non-cell autonomous multifactorial disease where a whole range of other cell types could contribute to the maintenance of motor neurons well being. Among them, glial cells, which surround motor neurons and provide nutritional and trophic support to them, could play a crucial role in disease pathogenesis (Philips & Rothstein, 2014).

Astrocytes are ectodermal cells involved in ion homeostasis, neurotransmitter recycling and metabolic support to surrounding neurons. One of the most important and extensively studied supportive functions of astrocytes is their involvement in the glutamate-glutamine cycle. Glutamate is one of the most important neurotransmitter in the central nervous system where it mediates excitatory synaptic communication between neurons. Uptake of glutamate from the synaptic cleft between presynaptic and postsynaptic neurons through glutamate transporters EAAT2 (GLT1 in rodents) and EAAT1 (GLAST in rodents) expressed by astrocytes will prevent excessive postsynaptic

stimulation of glutamate receptors and motor neuron cell death, a process which is called glutamate mediated excitotoxicity. Another important function of astrocytes is their involvement in the metabolic support of neurons. Astrocytes are tightly coupled to the bloodstream and strongly interconnected through gap-junctions through which they provide metabolic substrates over long distances. Under conditions of increased neuronal activity and metabolic substrate demand, astrocytes increase their glycolytic activity, converting glucose to lactate. Both glucose and lactate are distributed by astrocytes throughout the parenchyma and used as an energy substrate by neurons. When astrocytes encounter any biological hazard in their immediate surroundings, they become reactive and increase the expression of specific markers (e.g., glial fibrillary acidic protein: GFAP) in a process called astrogliosis. Astrogliosis is not mediated by resident astroglial cells proliferation but rather by activation of pre-existing resident astrocytes and by a change in their expression of proteins (e.g., increased GFAP, decreased GLT1) and altered morphology of their fine processes. In ALS patients, astrogliosis is seen both in the gray as well as the white matter of the brain; it is not limited to the motor cortex and to the ventral and dorsal horns of the spinal cord but spreads to the regions where the corticospinal tract fibers enter the gray matter in the spinal cord (Philips & Rothstein, 2014 and references therein).

The use of double transgenic GFAP-luc/SOD1 G93A mice carrying the non-pathogenic reporter transgene luciferase driven by murine GFAP promoter allowed the *in vivo* observation of astrogliosis establishment during ALS pathogenesis. The disease in mice is initiated simultaneously at the level of peripheral nerves and the spinal cord, and is characterized by several cycles of GFAP up-regulation. The first pathological increase in GFAP signals takes place around 25–35 days, when animals are asymptomatic, and is detectable both at the level of lumbar spinal cord projections and at the periphery. These early events are followed by several increases in GFAP promoter inductions, which is sharply activated at disease onset (85–90 days) (Keller et al., 2009). It has been shown that astrogliosis gradually increases with disease progression and differs in time course according to the SOD1 transgenic line under investigation and the expression levels of the transgene. Interestingly, the presence of reactive astrocytes increases not only in mutant SOD1 expressing mice but also in those expressing wild-type SOD1 at comparable levels at 40, 80 and 120 days despite disease progression (Alexianu et al., 2001).

Several studies have demonstrated that astrocytes expressing mutant SOD1 play an active role in ALS pathogenesis. In particular, it has been demonstrated that the

selective reduction of mutant SOD1 expression in astrocytes in SOD1 G37R (Yamanaka et al., 2008) or SOD1 G85R (Wang et al., 2011) transgenic mice or the transplantation of wild-type glial progenitor cells into the spinal cord of SOD1 G93A transgenic rats (Lepore et al., 2008) delays disease progression and extends survival.

Microglial cells are the resident immune cells of the central nervous system, of mesodermal origin, they represent the main immune-competent cells and the primary mediator of neuroinflammation of the central nervous system. In the normal adult nervous system, these cells exist in a resting state and are characterized by a small cell body and fine ramified processes. However, neuronal damage can rapidly activate the release of cytotoxic and inflammatory mediators. They closely interact with T-cells and astrocytes to mediate and regulate the inflammatory response; particularly, they release a whole range of pro-inflammatory or anti-inflammatory cytokines and chemokines when encountering any damaging hazard. They respond releasing pro-inflammatory factors (tumor necrosis factor alpha (TNFα), interferon-1β (IL-1β), nitric oxide (NO), O_2, and interferon-γ (IFN-γ)) to clear and/or limit biological hazards and subsequently they release anti-inflammatory factors (interleukin 4 (IL-4), IL-10, and insulin growth factor 1 (IGF1)) with the aim to repair the damage. In ALS patients as well as in ALS rodent models, there is a clear microglial reaction characterized by the upregulation of a whole range of microglial markers (CD11b, Iba1) and by the release of pro-inflammatory cytokines and chemokines (Philips & Rothstein, 2014 and references therein).

The analysis of microgliosis in the central nervous system of ALS patients largely depends on studies of postmortem tissues, which demonstrate increased microgliosis in the motor cortex, in the motor nuclei of the brain stem, in the corticospinal tract and the ventral horn of the spinal cord (Kawamata et al., 1992). Live in vivo PET scanning with 11C-PK11195, a ligand that highly binds to microglia, as well as other cells to a lesser extent, in the central nervous system revealed for the first time diffuse microgliosis in living ALS patients, and the results suggest a correlation between the extent of microgliosis and damage to upper motor neurons, but not lower motor neurons (Turner et al., 2004).

In either mutant SOD1 G93A or wild-type SOD1 transgenic mice, it has been shown that there is no increase in activated microglia in the spinal cord at 40 days of age. However, at 80 days, when mutant mice have minimal motor neurons loss and no clinical symptoms, extensive staining for microglia was observed in the ventral horn and proximal part of the anterior roots. Positive microglial staining, marked by the presence of round cell

bodies and thickened short ramified processes and multiple microglial processes, created a network around the motor neurons in the ventral horn gray matter. Interestingly, the expansion of the immune reaction correlates with disease progression in SOD1 mutant mice. In spinal cord sections, at all levels (sacral, lumbar, thoracic, or cervical), of transgenic mice expressing wild-type SOD1, microglial staining was minimal at all ages examined (40, 80, and 130 days) (Alexianu et al., 2001; Chiu et al., 2009).

To test the impact of microglia on ALS, mice expressing Cre driven by the myeloid CD11b promoter were generated and bred with floxed SOD1 G37R mice. The mutant Sod1 gene inactivation and mutant protein reduction in CD11b-positive cells prolonged survival by 99 days, slowing disease progression after onset, in Cre excised mice without affecting spinal cord microgliosis. This study sustains a role for activated microglia in the late stages of disease progression pointing out a role of these cells in motor neurons death. However, it is important to remember that CD11b is not specific to microglia in the central nervous system but it is also expresses by peripheral inflammatory myeloid cells and the Cre activation reduced mutant SOD1 expression also in these cells. Therefore it is possible to speculate that the slowing of later disease may derive in part from gene inactivation not just in microglia but also in peripheral macrophages or their progenitors and/or from the migration of those cells into the central nervous system after initial damage to motor neurons (Boillée et al., 2006). In fact, in mice expressing either mutant SOD1 G93A or SOD1 G37R a wide infiltration of macrophages in the peripheral nervous system accompanies axon degeneration in ventral roots, sciatic nerves, and muscle tissues. While in the spinal cord, the loss of motor neurons cell bodies induces the activation of resident microglia and infiltration of T cells, the peripheral nervous system denervation and degeneration of motor axons leads to significant peripheral macrophage activation. While microglia, in mutant SOD1 mice, are primarily tissue resident cells in the central nervous system, where they acquire dendritic cell surface receptors during disease progression, mainly acting as antigen-presenting cells to interact and activate T cells infiltrating the spinal cord; peripheral nervous system macrophages in ALS transgenic mice are mainly derived from the blood flow and their primary role in peripheral nerves may be the phagocytic removal of debris following axonal degeneration. Despite these functional differences, the immune activation in the central and peripheral nervous system follows similar kinetics. Interestingly, activated macrophages form cellular strands along the nerve, localized to spaces adjacent to axons and few macrophages were observed in the vicinity of end-plate neuromuscular synapses, at pre-symptomatic time points in

mutant SOD1 expressing mice but not in non transgenic and wild-ype SOD1 expressing ones. Following symptom onset, macrophage activation occupies a majority of the parenchyma. In the spinal cord, microglia is discretely activated in ventral horns at presymptomatic time points; following onset, glial activation becomes widespread and T cells infiltrate from the periphery (Chiu et al., 2009).

Figure 4

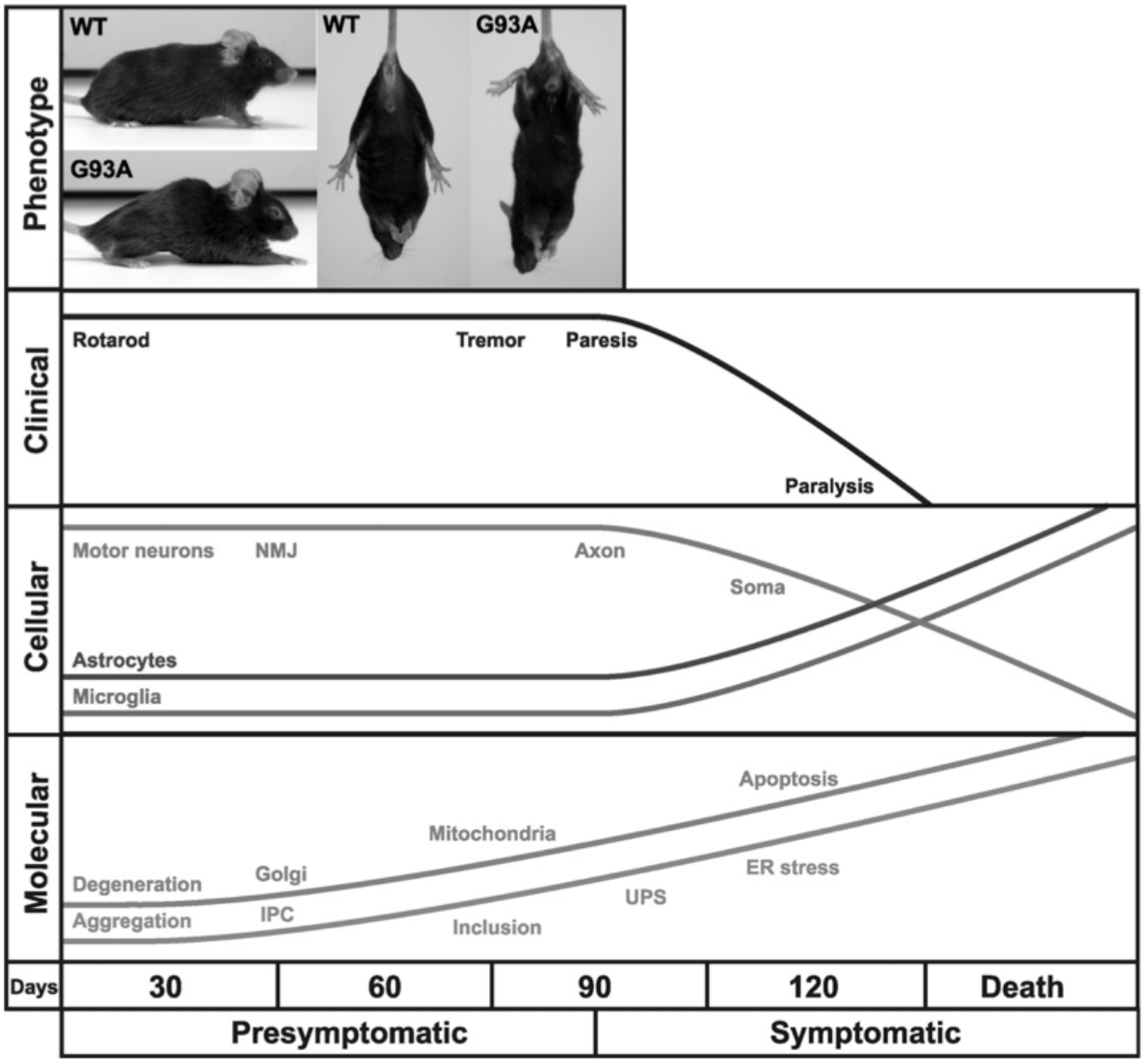

Figure 4: Summary of pathogenetic features identified in transgenic SOD1 G93A mice.
Mice develop evident locomotor deficits (hind limb tremor and weakness) around 3 months, and further progress to paralysis and premature death after 4 months.
Neuromuscular junctions degeneration appears around 47 days and is selective for fast-fatigable axons. Proximal axonal loss is prominent by 80 days coinciding with motor impairment and a severe 50% dropout of lower motor neurons is evident at 100 days. Spinal cords are also characterized by substantial astrocytosis and microgliosis around disease onset.
Hallmark pathologic features of spinal motor neurons also include mitochondrial vacuolization, Golgi apparatus fragmentation, neurofilament-positive inclusions and cytoplasmic SOD1-immunoreactive aggregates (modified from Turner & Talbot, 2008).

3.7 Altered neuronal excitability in ALS

Several studies, based on transcranial magnetic stimulation and cortical and peripheral neurophysiological investigations, demonstrated that ALS patients exhibit cortical hyperexcitability before any clinical sign of ALS or pathophysiological evidence of lower motor neurons dysfunction (Vucic et al., 2008; Vucic et al., 2013,b; Menon et al., 2014). Moreover, motor nerve excitability properties are strong predictors of survival in patients with ALS (Kanai et al., 2012). All these findings suggest that cortical dysfunction may precede the development of lower motor neurons dysfunction and lead to hypothesize that motor neurons degeneration in ALS may be mediated by cortical motor neurons hyperexcitability through an anterograde glutamate-mediated excitotoxic process: the so-called "*dying-forward*" hypothesis (Kiernan et al., 2011). At the basis of the neuronal hyperexcitability recorded in patients with suspected ALS and that subsequently developed the disease, it has been hypothesized that there could be both the degeneration of inhibitory cortical circuits (Thielsen et al., 2013) along with the release of high levels of extracellular glutamate (Vucic et al., 2013,b; Menon et al., 2014). However, it has been recently demonstrated that even motor neurons, differentiated from iPSCs generated from cells obtained in human ALS patients harboring SOD1, C9orf72 and FUS mutations, show signs of hyperexcitability. Interestingly, these neurons display a significantly higher action potential firing compared to those recorded in motor neurons differentiated from healthy subjects and in neurons where SOD1 A4V mutation was genetically corrected in the iPSC line, this phenotype was abrogated (Wainger et al., 2014).

Markedly elevated intrinsic electrical excitability was identified in cultured mice embryonic and neonatal dissociated spinal motor neurons expressing mutant SOD1 G93A. In particular, these motor neurons did not show any differences in the resting potential, in the input conductance, in the action potential shape and in the after hyperpolarization amplitude, between G93A and control motor neurons. However, the maximal firing rate of those expressing SOD1 G93A was much greater than in the control ones in presence of ionotropic receptors blockers; assuring that these differences were not due to alterations in spontaneous synaptic inputs (Kuo et al., 2004; Kuo et al., 2005; Pieri et al., 2009; Schuster et al., 2012; Martin et al., 2013). Similar results were obtained comparing hypoglossal motor neurons and spinal cord interneurons electrical properties of mutant human SOD1 G93A expressing mice with those recorded in wild-type human

SOD1 expressing mice and non transgenic mice in acutely prepared slice at P4-P10 or P10-P12. In this way, it was demonstrated that neuronal hyperexcitability was specifically due to the expression of the mutated SOD1 G93A protein but not of wild-type SOD1 and that even interneurons present hyperexcitability, which may contribute to neuronal loss at later stages in the pathology (Van Zundert et al., 2008). Evidence that neuronal hyperexcitability is not a peculiar feature of ALS pathology associated to SOD1 mutations, were obtained not only by Wainger and colleagues in iPSCs derived from patients with ALS associated to different mutated genes (Wainger et al., 2014) but also by the studies conducted in the wobbler mouse, an ALS model carrying a point mutation in the Vps54 gene. This gene encodes a protein involved in retrograde transport from both early and late endosomes to the trans Golgi network. These animals exhibit signs of cortical and hippocampal excitability already in the presymptomatic phase of the disease with a concomitant reduction in inhibitory paravalbumin positive interneurons in the symptomatic stage of the disease (Thielsen et al., 2013).

Beyond the excitation/inhibition unbalance hypothesized to be at the basis of neuronal hyperexcitability (Vucic et al., 2009) several authors observed the increased activity of the persistent (non-inactivating) sodium current I_{NaP} in acute brain slice and cultured neurons obtained form mice expressing human SOD1 G93A mice (Kuo et al., 2005; Van Zundert et al., 2008; Pieri et al., 2009). The voltage-dependent activation threshold and the peak potential of the I_{NaP} result to be similar in wild-type and G93A neurons; however, I_{NaP} amplitude measured at the peak of Current/Voltage relationship and the current density is significantly higher in G93A neurons (Pieri et al., 2009). Although I_{NaP} represents a small fraction of the total neuronal current (0.8-1%), it can profoundly affect neurons and network behavior. This current, in fact, enhances neuronal excitability near firing threshold and is essential for spikes generation during sustained inputs (Urbani & Belluzzi, 2000). Since I_{NaP} can be activated close to the cell's resting potential, small increases in this current can enhance cell intrinsic excitability, alter spike initiation and amplify the firing rate. In addition, the excitatory synaptic inputs received by a given neuron can be greatly amplified and prolonged by I_{NaP} thereby impacting the neuron's output by increasing its firing rates in response to synaptic modulation (Urbani & Belluzzi, 2000; Van Zundert et al., 2012)

Interestingly, riluzole, the only drug approved for the treatment of ALS patients as capable to slow disease progression (Bensimon et al., 1994), has been demonstrated to be a selective blocker of I_{NaP} at low concentrations (Urbani & Belluzzi, 2000) and proved to

be able to markedly block I_{NaP} and rapidly decrease firing frequency both in wild-type and mutant SOD1 expressing neurons (Kuo et al., 2005; Pieri et al., 2009). These evidence are of the outmost importance because the mechanism of action by which riluzole exerts its therapeutic effects is complex and still not completely understood; it involves the inhibition of the voltage-dependent sodium channels and also a reduction of glutamate release although, the correlation of the two mechanisms remains to be elucidated because tetrodotoxin, a sodium channel blocker, fails to mediate the same effect on glutamate release (Urbani & Belluzzi, 2000).

Several studies also show that altered neuronal electrical properties are associated with morphological defects (Van Zundert et al., 2008; Amendola & Durand, 2008; Martin et al., 2013). It has been observed that human SOD1 G93A expressing mice embryonic spinal motor neurons (Martin et al., 2013) and P6 hypoglossal motor neurons (Van Zundert et al., 2008), in addition to hyperexcitability, show a significant reduction in the terminal dendritic arborization. In the latter case, significantly fewer dendrites cross the midline into the territory of contralateral hypoglossal motor neurons compared to control littermates and these abnormalities are accompanied by a transient delay in the development of the gross locomotor ability of the forelimbs (Van Zundert et al., 2008). On the contrary, lumbar motor neurons expressing SOD1 G85R, showing hyperexcitability, present a significant increase in the total dendritic length, in the dendritic arborization surface area and in the total number of axonal branches (Amendola & Durand, 2008). However, it is still unknown whether the morphological alterations are the cause or the consequence of changes in neuronal excitability.

4. ZEBRAFISH MODELS OF HUMAN MOTOR NEURON DISEASES

Motor neuron diseases constitute an expanding, heterogeneous group of developmental and neurodegenerative disorders anatomically subdivided according to their involvement of upper motor neurons or lower motor neurons or both. The upper motor neurons of the central nervous systems originate in the motor cortex and deliver motor information to the lower motor neurons. Lower motor neurons are located in the cranial motor nuclei in the brainstem and spinal cord and drive impulses from the upper motor neurons to the skeletal muscles at neuromuscular synapses. Symptoms associated to upper motor neurons dysfunction generally include weakness, speech problems, overactive tendon reflexes, spasticity, Babinski sign, clonus, and inappropriate emotionality while lower motor neurons degeneration causes weakness, attenuated reflexes, cramps, twitching, and muscle wasting. Unfortunately, considerable overlaps of clinical and pathophysiological features complicate the precise diagnosis of these diseases in patients and raises controversies about the disorders classification. Animal models of human motor neurons diseases, mostly rodents, but also the fruit fly (*Drosophila melanogaster*) and the nematode worm (*Caenorhabditis elegans*), have been used in the attempt to understand the neurobiological basis of these pathologies and to predict successful treatment strategies (Babin et al., 2014).

The zebrafish (*Danio rerio*) is a vertebrate species, with a nervous system organization similar to humans, increasingly used to model human diseases. It represents a powerful experimental model for the study of disorders affecting the nervous system and of physiological processes involved in nervous system morphogenesis and maintenance due to the high conservation of genes implicated in neurodegenerative diseases. The zebrafish model presents many methodological advantages and extensive collections of useful resources (zfin.org web site). These include tools applicable *in vivo*, like whole-mount imaging thanks to the optical transparency of zebrafish embryos and early larval stages, methodologies for modulating gene expression, behavioral tests to examine changes in motor activity and simplified simultaneous chemical/drug testing on large number of animals. The fully sequenced genome is available, together with molecular anatomical atlases and collections of transgenic lines expressing fluorescent proteins under neuron-specific promoters. Numerous gene knockout lines and their short-term associated phenotypes are now complementary to antisense morpholino oligonucleotides (AMO) transitory knockdown and other genome editing methods like transcription

activator-like effector nucleases (TALEN) and the CRISPR/Cas system and transgenic techniques for conditional gene activation or inactivation. In addition to the many genetic tools available, behavioral genetics are easily accessible in zebrafish: its stereotyped movement patterns and tactile response abilities may be used to model some of the molecular, electrophysiological, and behavioral aspects of neural diseases. Moreover, the zebrafish model has become an attractive alternative to rodents, in the attempt to develop high-throughput screenings to identify genetic interactions or small molecules with toxic or therapeutic effects, thanks to lower costs and less time-consuming experiments (Kabashi et al., 2010,a; Babin et al., 2014).

4.1 Comparative neuroanatomy of human and zebrafish motor systems

Vertebrate motor system is hierarchically organized in three levels of control: motor cortex, brainstem, and spinal cord. Zebrafish share this organizational structure and have at least twenty different neuronal populations in the brain involved in the control of locomotion, mostly located in the brainstem and projecting to the spinal cord. While the brainstem organization of neurons with descending axons is highly conserved among other vertebrates, including zebrafish, an important difference between teleost fish and mammals is that they do not have direct telencephalic projections to the spinal cord, probably because the corticospinal tract in mammals is an adaptation for the fine motor control of the limbs (Babin et al., 2014 and references therein). Therefore, the zebrafish model represents a valuable system to investigate pathologies affecting spinal circuits but less suitable to study disease mechanisms involving the motor cortex.

Spinal cord

The human motor nuclei in the spinal cord are arranged along a medial-lateral axis according to their function. The ventral medial motor column projects to the axial muscles in the neck and back, the hypaxial (ventral) motor column projects to the hypaxial muscles in the ventral body wall, and the dorsal lateral motor columns project to the limb muscles. This topographic map of spinal cord motor nuclei, arranged in different motor columns innervating different groups of muscles is present in mammals, reptiles and birds, but not in other vertebrates like fish. Spinal motor neurons can be distinguished in alpha motor

neurons (α-MNs) innervating extrafusal muscle fibers and driving muscle contraction and gamma motor neurons (γ-MNs) innervating intrafusal muscle fibers of the muscle spindle and involved in proprioception. α-MNs, the most abundant class of spinal motor neurons, can in turn be classified in three subtypes, according to the contractile properties of the motor units that they form with target muscle fibers: slow-twitch, fatigue resistant (S); fast-twitch, fatigue resistant (FR); fast-twitch, fatigable (FF) (Babin et al., 2014). Motor neurons of the FF-subtype have large cell bodies and large-diameter, fast-conducting axons and seem to be the most sensitive to degenerative disorders and aging, while the S-subtype has the smallest cell bodies and axons and are more resistant to degeneration (Pun et al., 2006).

Zebrafish spinal motor neurons are located in the motor columns in ventral horns of the spinal cord and may be divided into primary and secondary classes, according to when they differentiate and innervate their target musculature. Primary motor neurons (PMNs) are larger, appear during gastrulation and undergo axonogenesis during the first day of development. Three to four individual PMNs may be identified in each spinal hemisegment by their head-tail positions, axonal trajectories, and electrical membrane properties. Caudal primary motor neurons (CaP) innervate the ventral trunk musculature, middle primary motor neurons (MiP) innervate dorsal trunk musculature, and rostral primary motor neurons (RoP) innervate muscle fibers in between. A fourth class, variable primary motor neurons (VaP) innervating muscle fibers located between the territory of rostral and middle primary motor neurons can be identified, although they typically undergo apoptosis by 36 hours post fertilization (hpf). Secondary motor neurons (SMNs), located more ventrally in the motor column, are smaller, more numerous, appear later in development, and typically have thinner axons than PMNs (Figure 5). PMNs have not been described in amniotes, thus human α-MNs may be more similar to SMNs. No γ-MNs have been described in zebrafish, which do not have intrafusal muscle fibers (Babin et al., 2014 and references therein; Drapeau et al., 2002).

Skeletal muscle

Axial motor structures form the primitive motor apparatus of vertebrates and consist of a rostro-caudal series of myomeres. This myomeric musculature is also present in most anamniotic vertebrates, including zebrafish (Babin et al., 2014). In adult zebrafish, slow and fast muscle fibers occupy distinct regions of the axial muscle. Fast muscle fibers

represent the deep and large portion of the ventral and dorsal myotomes, while slow muscle fibers are segregated into a lateral wedge-shaped region of the myotomes at the level of the horizontal septum, which separates the ventral (hypaxial) and dorsal (epaxial) muscles. In addition, there are intermediate muscle fibers located between the slow and fast muscle fibers (Ampatzis et al., 2013). Slow fibers, forming the superficial monolayer on the surface of the myotome, are well-equipped for oxidative phosphorylation and are resistant to fatigue, while fast fibers, in the deep portion of the myotome, are more fatigable as they rely on anaerobic glycolysis for ATP generation (Drapeau et al., 2002; Brustein et al., 2003). Each fast fiber is innervated by a single PMN and up to 4 SMNs, whereas each slow fiber is innervated by several SMNs. The two groups of fibers can be differentially controlled and perform different functions: slow fibers are activated during slow sustained swimming, whereas fast fibers only become active during rapid swimming or escape movements. Electrophysiological evidence indicate that slow fibers are tonic fibers, homologous to the tonic fibers described in the mammalian extra-ocular muscle and, therefore, they cannot be considered the homologs of mammalian slow twitch muscle, while fast fibers are a twitch-fiber type. Skeletal muscle fibers in zebrafish share many molecular and histological features with mammalian muscle fibers, including preservation of the components of the dystrophin-associated glycoprotein complex, the excitation-contraction coupling machinery and the contractile apparatus (Babin et al., 2014 and references therein).

4.2 From cells to circuits: development of the locomotor network in zebrafish spinal cord

As a result of the many similarities of the locomotor network organization, that have been described from invertebrates to vertebrates, including mammals; the zebrafish is a useful system for gaining new insights into the development of the neural control of vertebrate locomotion. The attractiveness of the zebrafish as a model for developmental studies stems from the ease of obtaining large numbers of embryos that are transparent for microscopic observations: a pair of zebrafish simultaneously lays and externally fertilizes 100–200 eggs, and the small embryos (1 mm in length) develop rapidly with stereotyped stages and hatch after only 2 days (52 hpf) (Kimmel et al., 1995).

The stereotypic motor activity of the developing zebrafish includes three sequentially appearing behaviors: a transient period of alternating tail coilings followed by

responses to touch and the appearance of organized swimming (Drapeau et al., 2002; Brustein et al. 2003).

Spontaneous coiling

The nervous and muscular systems must develop and function in concert to bring about proper locomotion. Zebrafish neurogenesis in the spinal cord starts 6 hpf, during gastrulation, when sensory neurons, interneurons and primary motor neurons differentiate from precursors located respectively in the dorsal, medial and ventral longitudinal columns of the spinal cord (Drapeau et al., 2002; Lewis et al., 2003).

Muscle development starts 11 hpf in rostral somites, when medial paraxial mesodermal cells differentiate into adaxial muscle precursor cells. One population of adaxial cells maintains its medial location and develops into the first contractile myotomal fibers: the “muscle pioneers” while a second population of adaxial cells migrates laterally where they elongate and form the mononucleate superficial embryonic slow red muscle (ER) fibers. Lateral paraxial mesodermal cells later differentiate into lateral presomitic muscle precursor cells, ultimately forming the multinucleate embryonic fast white (EW) fibers that constitute the bulk of the myotomal muscle. When embryonic myotomal segments first form, they are block shaped with ER and EW fibers running parallel to the notochord. Within a few hours, the deeper EW fibers take on their characteristic oblique chevron-shaped (<) orientation and ER fibers retain their parallel orientation forming a blanketing layer of approximately 30 fibers per segment. At the time of the first contractions, only two fiber types are present: the ER and EW fibers and the anatomical organization of the myotomes of developing embryos and larvae is much simpler than that of the adult. Primary motor neurons start transmitting inputs to muscle pioneers and soon afterwards EW fibers are innervated. At this stage of development, ER and EW fibers have an extensive electrical coupling (ER–ER and EW–EW but not ER–EW), forming a contractile syncytium in the embryo that decreases greatly by hatching at 52 hpf. At the onset of motor neurons axon outgrowth, the trunk of zebrafish embryos contains approximately 16 myotomes. Each side of the spinal cord segment, within each myotomal division, usually contains three individually identifiable primary motor neurons (PMNs). The first PMN to send an axon out of the spinal cord (pioneering the ventral root) after 17 hpf is the caudal primary motor neuron (CaP). In the next 1–2 hours the CaP axon is followed in sequence by the axons of the middle primary neuron (MiP) and the rostral primary neuron

(RoP). The CaP, RoP, and MiP axons, respectively innervate the ventral, lateral, and dorsal muscle of the overlying myotome. This innervation pattern is exclusive to each region and the different growth cones follow stereotypical pathways. All three primary motor neurons axons follow a common pathway on the medial surface of the myotome until they reach adaxial muscle pioneers at the developing horizontal myoseptum. These muscle pioneers seem to act as choice points as the axons pause at their contact and then diverge to follow their final innervation patterns. In taking this common path, the primary motor neurons pioneer the peripheral motor nerve. Ten hours after this initial axonogenesis (26 hpf), a new wave of outgrowth by secondary motor neurons begins, with about two dozen secondary motor neurons per segment sending axons out of the spinal cord through the common ventral root and branching into the muscle mass (Drapeau et al., 2002; Lewis et al., 2003).

Spontaneous alternating side-to-side contractions of the trunk (coils) appear 17 hpf. These movements are not myogenic and originate from the spinal cord, since they depend on functional motor neurons innervation and persist in the isolated trunk independently of supraspinal inputs (Saint-Amant & Drapeau, 2000; Saint-Amant & Drapeau, 2001; Drapeau et al., 2002). At onset of spontaneous coiling only four types of spinal neurons are active: three types of interneurons: ipsilateral caudal (IC), ventrolateral descending (VeLD), and commissural primary ascending (CoPA) interneurons and motor neurons. Around 17 hpf, these neurons show ‘‘periodic depolarizations’’, rhythmic membrane oscillations (with a frequency around 0.6 Hz) that are resistant to block of neurotransmitter receptors (Saint-Amant & Drapeau, 2000). By 20-21 hpf, periodic depolarizations become interspersed with ‘‘synaptic bursts’’ that comprise periodic depolarization-bursts evoked by glycine released from newly integrated neurons (Saint-Amant & Drapeau, 2000; Saint-Amant & Drapeau 2001; Tong & McDearmid, 2012). The periodic depolarizations appear early in development, 17–20 hpf, and are slow, sustained depolarizations that trigger action potentials and presumably generate the coils, while bursts of glycinergic inputs arise later, after 21 hpf, and consist of rapid synaptic events. Surprisingly, during the period of spontaneous coiling the neural activity is exclusively based on electrical coupling among cells, in fact, the blockade of receptor channels commonly found in the larval spinal cord (Glycine receptors, AMPAR, NMDAR, AChR, GABA receptors) does not impair coils and persists when all chemical synaptic transmission is abolished with botulinum toxin. However, uncouplers of gap junctions suppress the activity, indicating that a different mechanism of network activation is at play at this stage of development (Saint-Amant &

Drapeau, 2001). In vivo electrophysiology experiments allowed to determine that periodic depolarizations depend upon a persistent sodium current (I_{NaP}). This current, often implicated in pacemaking, mediates spontaneous depolarizations in the subset of zebrafish active interneurons and motor neurons and promotes the generation of slow membrane voltage oscillations during spontaneous coiling. The administration of 5 μM riluzole inhibits I_{NaP} and, without affecting spike amplitude or rheobase, gradually abolished periodic depolarizations. Since 5 μM riluzole similarly blocks coiling behavior in freely moving embryos, it suggests that I_{NaP} drives coiling activity (Tong & McDearmid, 2012). The role of the glycinergic bursts at 21 hpf is still not clear since blocking glycinergic synapses with strychnine had little effect on the coiling behavior. However, it was observed that periodic depolarizations on one side of the trunk occurred simultaneously with glycinergic bursts on the other side (Saint-Amant & Drapeau, 2001).

An important role for electrical coupling, in developing central networks, has been suggested for many vertebrates where it is implicated in the formation of chemical synapses. Interestingly, electrical coupling is a fundamental mechanism of synchronization in central program generators of invertebrate nervous systems and precedes the appearance of chemical transmission. It has been therefore suggested that the electrically coupled network of the zebrafish embryo could be a fundamental, phylogenetically conserved, scaffold for synchronizing early rhythmic networks (Drapeau et al., 2002).

Touch response

At the peak of the spontaneous tail coilings (19 hpf) the zebrafish embryos do not respond to touch. Starting from 21 hpf the embryos could respond to touch with an over-the-head, fast coiling of the trunk; however, a mature response to touch behavior appears only 27 hpf when touching the head results in a full coiling response whereas, touching the tail now results in a partial coil that, for the first time, elicits brief swimming episodes in dechorionated embryos. At this developmental stage, touching the head presumably activates trigeminal sensory neurons whereas, touching the tail activates spinal Rohon–Beard sensory neurons, which both project to the hindbrain and innervate reticulospinal Mauthner neurons that send projections to the spinal cord. These responses require an intact hindbrain in addition to the spinal cord and suggest that the new behaviors are related to a functional rearrangement in the hindbrain or spinal cord circuitry, or perhaps both. While an electrically coupled network of a subset of spinal neurons generates coiling

contractions, a chemical (glutamatergic and glycinergic) synaptic drive underlies touch responses and swimming. Because the hindbrain is required for the touch response and most reticulospinal neurons are glutamatergic, part of the newly functional glutamatergic synapses are likely to be descending projections from the hindbrain reticulospinal neurons (Brustein et al., 2003; Knogler et al., 2014).

The appearance of the touch evoked motor response is characterized by the development of neuromuscular synaptogenesis. Neuromuscular synapses are first formed on “muscle pioneer” at the choice point and on muscle fibers that are dorsally and ventrally adjacent to them, on the medial surface of the myotome, between 20-28 hpf. AChRs are clustered beneath outgrowing motor axons but they are still not precisely associated with presynaptic vesicles clusters in nascent presynaptic terminals. By 48 hpf, motor axons extend branches into the myotomes, form synapses with laterally located muscle fibers, turn laterally at the edge of the myotome and grow along and innervate the myosepta. In contrast to earlier developmental stages, now presynaptic terminals are almost always apposed to AChR clusters. By 120 hpf, the number of synapses further increases and synapses become distributed throughout the entire myotome (Panzer et al., 2005).

Swimming

At early larval stages, 3 days post fertilization (dpf), zebrafish are generally inactive and display only occasional episodes of spontaneous “burst” swimming and, only by 4 dpf, a more directed “beat-and-glide” swimming pattern appears. At this stage, only embryonic muscle fiber types are developed and a primary myotome is formed by fast muscles fibers (EW) and by only a superficial monolayer of slow muscle fibers (ER). As the zebrafish matures to the juvenile and the adult stages, the swimming activity increases and now the locomotor pattern changes to “slow-continuous” swimming. This change in the motor pattern is accompanied by the development of intermediate and adult slow red fibers (Ampatzis et al., 2013). The myotome morphology changes dramatically from the simple chevron (V) shape of the embryo to the complicated (W) shape of the adult myotome that is optimized for power production during undulatory swimming (Drapeau et al., 2002). The trunk musculature in the adult zebrafish thus contains three types of muscle fibers with a specific arrangement into three discrete compartments: superficial slow fibers, an adjacent area of intermediate fibers, and more medially, the larger part of the myotomes with fast fibers (Figure 5). The developmental changes in the muscle organization are associated

with a refinement of motor neurons organization. In larval zebrafish, only fast muscles are developed and they are innervated by early-developed fast primary motor neurons and fast secondary motor neurons to produce motion geared for fast swimming and escape. At these early stages of development, the motor column extends only dorsoventrally in the spinal cord, is only 1–2 cell bodies thick and there are no motor neurons segregation into distinct pools as they innervate only fast muscles. The picture changes in the adult zebrafish, where the intermediate and slow muscles are fully developed and the motor column extends laterally and more ventrally in the spinal cord. The organization of motor neurons switches from the larval continuous pattern into segregated pools of motor neurons displaying distinct anatomical and physiological properties with a clear somatotopic organization pattern related to the type of muscle they innervate. Specifically, fast secondary motor neurons are shared between the escape and swimming circuits, slow and intermediate secondary motor neurons are only used for swimming, and fast primary motor neurons are used only for escape (Figure 5) (Ampatzis et al., 2013). The study of the neurotransmitters involved in the development of swimming behavior shows that a rhythmic glutamatergic synaptic drive to motor neurons during locomotion in combination with reciprocal glycinergic inhibition plays a major role in the generation of rhythmic locomotor alternations; however, swimming becomes sustained in larvae once the neuromodulatory serotonergic system develops (Brustein et al., 2003 and references therein).

Figure 5

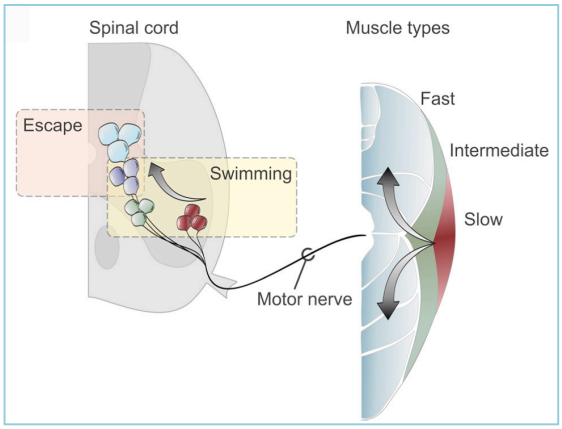

Figure 5: Schematic representation of adult zebrafish motor neurons pools in the spinal cord and muscle types organization in lateral body wall. Motor neurons innervating slow (red), intermediate (green), and fast (blue) muscles are organized somatotopically in different parts of the spinal motor column. Swimming activity is mediated by the recruitment of the late-developed slow (red) and intermediate (green) secondary motor neurons, the early-developed primary (cyan) motor neurons do not participate in swimming and are only active during escape while early-developed (fast) secondary motor neurons (purple) contribute to both motor responses (modified from Ampatzis et al., 2013).

4.3 Zebrafish Sod1 G93R: a genetic model of ALS

The first stable transgenic zebrafish lines expressing either a wild-type (wtSod1) or a mutant form of Sod1 (mSod1) were generated in the laboratory of Dr. Christine E. Beattie. Because zebrafish live at a lower temperature (28°C) than mammals (37°C), the zebrafish *sod1* gene and regulatory regions were used to generate the transgenic animals, in order to avoid any adverse effect of temperature on the enzyme functionality. Both transgenic zebrafish lines were generated injecting into one-cell fertilized embryos a DNA construct composed by a 21-kb zebrafish genomic region containing the endogenous *sod1* gene (5.06 kb) and *sod1* promoter and flanking sequences (11.7 kb upstream and 4.5 kb downstream) followed by the zebrafish *heat shock protein 70* (hsp70) promoter driving the expression of the fluorescent protein DsRed, for the identification of the transgenic fish. They characterized a wtSod1 line containing ~42 copies of the wild-type form of the *sod1* gene and a mSod1 line that integrated a higher number (~165 copies) of mutated *sod1* gene (348 G>C; NCBI Reference Sequence NP_571369.1), overexpressing a mutated form of the Sod1 protein where the glycine 93 is changed to arginine (G93R) (Ramesh et al., 2010).

This mutation affects an evolutionarily conserved amino acid that is mutated in FALS and that is associated to a disease with a precocious onset in humans (Elshafey et al., 1994; Orrell et al., 1999). The substitution of the glycine in position 93 with an arginine in the human SOD1 aminoacidic sequence generates a wild-type like protein. Since this substitution occurs distally to the dimer interface, it is believed that this mutation critically impairs the capability of the protein to maintain the native structure (Durazo et al., 2009).

Both transgenic zebrafish lines are characterized by an ubiquitous overexpression of Sod1, consistent with the expression profile of the endogenous *sod1* gene and, in particular, by a threefold increase in the steady-state Sod1 protein levels in the brain and a fourfold increase in the spinal cord, at one year of age, compared with non-transgenic siblings. At 18 months of age, Sod1 G93R zebrafish exhibit a short survival in comparison with wtSod1 and non-transgenic zebrafish. At the end-stage of the pathology, adult zebrafish overexpressing Sod1 G93R present spinal cord motor neurons loss and show shrunken spinal motor neurons containing vacuolated mitochondria with disorganized cristae and myofibrillar degeneration and extensive collagen deposition in fast trunk muscle at the ultrastructural analyses. At 12 months of age, Sod1 G93R expressing zebrafish display endurance impairment in swimming against an increasing current over

time in the tunnel-swimming test, and neuromuscular junctions defects, already present 11 days post fertilization (Ramesh et al., 2010).

This zebrafish model harbors a fluorescent heat shock stress response (HSR) reporter gene: the fluorescent protein DsRed under the control of *hsp70* promoter. The HSR is an endogenous cellular pathway that attempts to refold the damaged proteins in stressed cells through the activation of genes capable to assist protein folding. One of the gene expressed in this response is that encoding for Hsp70. Since protein misfolding is one of the contributing mechanisms to neuronal toxicity in ALS, Sod1 G93R protein misfolding in vulnerable cell populations would cause cellular stress and activate HSR allowing the identification of potentially dysfunctional neurons thanks to DsRed expression. The HSR, in Sod1 G93R zebrafish, was first observed 24 hpf in inhibitory glycinergic interneurons and *in vivo* patch clamp recordings revealed that HSR was followed by a reduction in glycine release 96 hpf. The loss of inhibitory inputs contributes to the onset of motor neurons stress, which is observed in Sod1 G93R zebrafish at 6 months of age and interestingly, motor neurons showing the HSR are those mainly associated with a significant reduction in neuromuscular junctions volume. Riluzole treatment of 24 hpf mutant transgenic embryos for 4 days caused a dose-dependent reduction in DsRed fluorescence in embryos (McGown et al., 2012).

These evidence show that the Sod1 G93R zebrafish represent a powerful tool to study ALS since it develops hallmark features of the disease commonly associated with both murine models and human disease. Zebrafish experimental accessibility, small size, and the possibility to implement drug or genetic screening platforms, based on zebrafish embryos and larvae, make this animal a good complement to other vertebrate models of the disease and therefore we need to deepen our knowledge on Sod1 G93R zebrafish ALS pathophysiology.

AIMS OF THE WORK

Sod1 G93R zebrafish is a very promising animal model for the study of pathogenetic mechanisms and therapies related to ALS, even if the characterization of this model is still in its early stages. In previous research zebrafish Sod1 G93R has been used to study such disease aspects as motor neurons degeneration and locomotor impairments, although Sod1 G93R zebrafish awaits further exploration for the realization of its full potential as an animal model in the development of drugs and genetic screenings.

The first aim of this work is to precisely characterize the disease phenotype in adult zebrafish overexpressing both mutant Sod1 (mSod1) and wild-type Sod1 (wtSod1) in order to identify alterations associated with the overexpression of Sod1 in both mutant and wild-type as compared to control zebrafish.

We have studied all the main pathological events occurring in ALS, that have already been well identified and documented in humans and other models of the disease, in the adult zebrafish model: locomotor impairments, motor neurons degeneration and spinal cord atrophy, neuromuscular junctions loss, muscle fibers atrophy, ultrastructural alterations at the nerves terminals and muscles. Moreover, we have assessed the involvement of astrocytes, microglia and peripheral inflammatory cells. We have characterized these events along the entire body of the animal in order to evaluate the alterations associated with the disease and how these alterations affect the entire trunk of the animal and/or specific areas.

Following our completion of the adult pictures of the disease, we have searched for precocious ALS hallmark features in zebrafish embryos and larvae. Exploiting the optical transparency of zebrafish embryos at early larval stages has allowed us to perform whole-mount immunofluorescence staining from which we were able to study the overexpression of the wild-type or mutant Sod1 effects on spinal motor neurons development and neuromuscular junctions maturation, already at precocious developmental stages. Furthermore, we have performed behavioral tests in order to examine changes in motor activity on zebrafish embryos and larvae: in particular we have evaluated whether the expression of mutant Sod1 impairs spontaneous coiling 20 hpf, touched evoked tail coiling response 48 hpf and the burst swimming response 96 hpf.

We have investigated spinal neurons electrical properties of mSod1 expressing zebrafish embryos, thanks to a genetically encoded FRET-based voltage biosensor.

By administering riluzole directly into the embryo water we tested for the possibility of pharmacological modulation of precocious alterations associated to the mutant Sod1 expression.

This series of experiments have allowed us to understand how zebrafish embryos and larvae expressing mutant Sod1 G93R are powerful models for the development of high-throughput screenings to study genetic interactions and identify small molecules with toxic or therapeutic effects.

We conclude that the zebrafish Sod1 G93R is a valuable complement to other animal models and is potentially a powerful model on its own in the study of ALS due mainly to its advantages as an imaging tool, particularly in early developmental stages, and its rapid maturation rate, not to mention other economic advantages related to cost, maintenance and study duration.